Chapter 3

Novel quinoline derivatives containing substituted DHPM hybrids, *In Vitro* Antimicrobial Assessment and Corresponding *In Silico* Analysis

3.1 Introduction

One-pot multicomponent reactions represent a potent synthetic strategy and versatile method for the synthesis of diverse types of molecules with extensive applications.[72] The growing interest in multicomponent reactions stems from their inherent advantages for synthetic chemists compared to traditional linear synthesis, which include straightforward operation, uncomplicated starting materials, elevated product complexity, and extensive product diversity.[73,74] The three-component one-pot Biginelli reaction is among the processes utilized in the synthesis of heterocycles. The amalgamation of aldehyde, urea or thiourea derivative, and active methylene molecule results in the synthesis of dihydropyrimidine (DHPM), a category of organic compounds extensively utilized in medicine for their diverse biological activities.[75] Their success in medicine is attributed to the multicomponent character of such reaction, which facilitates the incorporation of diverse pharmacophoric groups into the structure of dihydropyrimidines.[76-79] Pyrimidine moiety is an important class of nitrogen containing heterocycles[80] and is widely used as a key building block for pharmaceutical agents. Its derivatives exhibit antibacterial (**1**), antifungal (**2**, **3**)[81] analgesic (**4**),[82] calcium antagonist,[83] anti-inflammatory (**5**)[84] and anti-tumor activity (**6**, **7**).[85] In addition, several marine natural products with interesting biological activities containing pyrimidine core have recently been isolated.[86]

The extensive utilization of dihydropyrimidines has motivated researchers to enhance their chemistry by broadening the array of building blocks in the Biginelli reaction.[87] The examination of changed compounds and structure-activity relationships facilitate a comprehensive understanding of the stereochemical conformational prerequisites for activity, which are heavily influenced by the dynamism of performing diverse interactions, such as intra molecular hydrogen bonds within the structure.[88] On the other hand, quinoline is mainly used in the production of various speciality chemicals, which provide a wide variety of applications,

onto which several industrial sectors rely. In addition to this, quinoline has established anti-malarial derivatives (**8**, **9**), including quinine, chloroquine, amodiaquine and primaquine.[89]

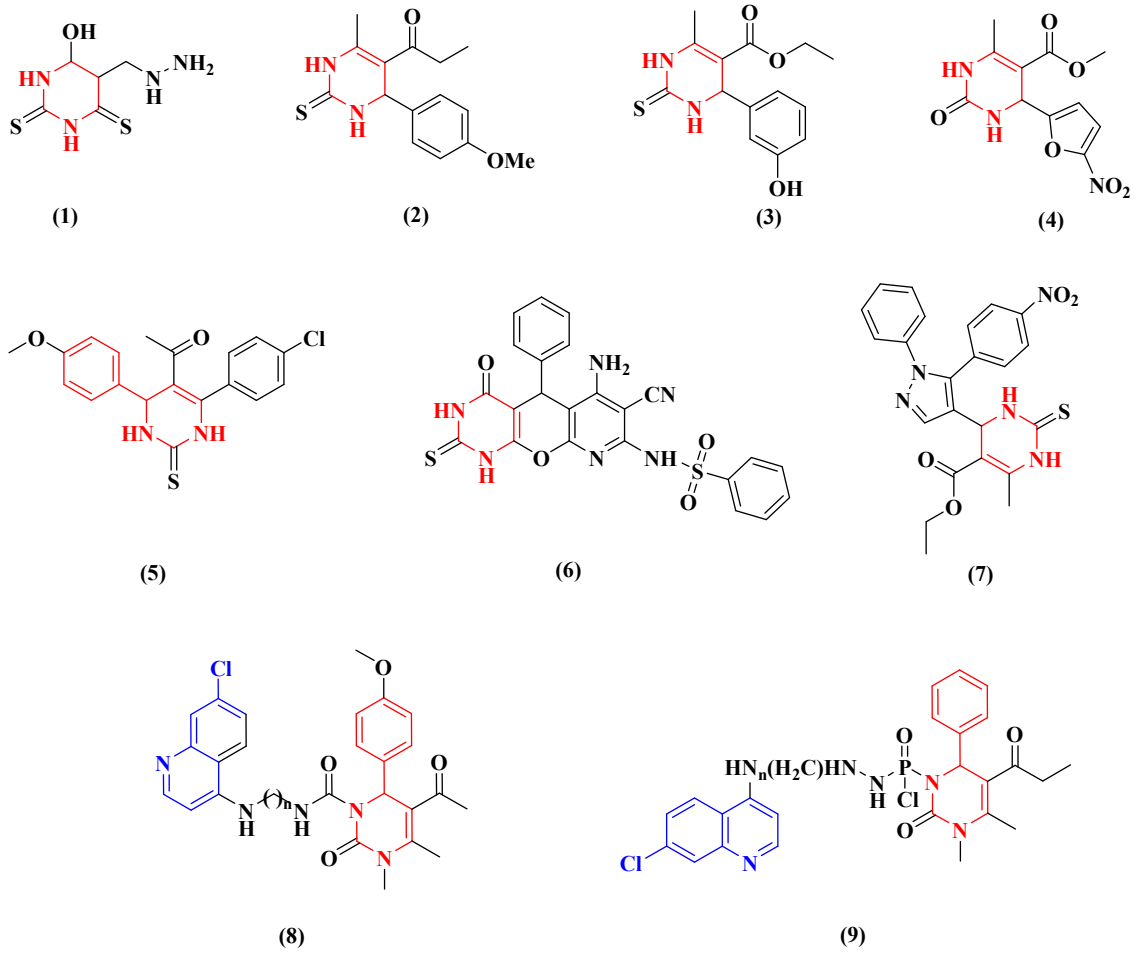

Figure 1: Some bio-active quinoline & DHPM derivatives.

3.1.1 Synthetic methodologies for the substituted quinoline-DHPM framework and its biological significance

A combination of *N*-phenylacetoacetamide (**1**), an aromatic aldehyde (**2**) and urea or thiourea (**3**), cupric chloride (10 mmol), and 2–3 drops of concentrated hydrochloric acid (HCl) was triturated and combined to produce a syrup in a solvent-free environment then kept overnight. The contents were exposed to ice-cold conditions. Poured onto the water and the resultant product were filtered, dried and solidified (**4**). All derivatives interact with rRNA present in both Gram-positive and Gram-negative organisms. Most of the substances depicted

antineoplastic activity as predicted by PASS biological activity assessment. The developed compounds might serve as potential antibacterial inhibitors and have prominent anti-neoplastic activity (**Figure 3.1**).[90]

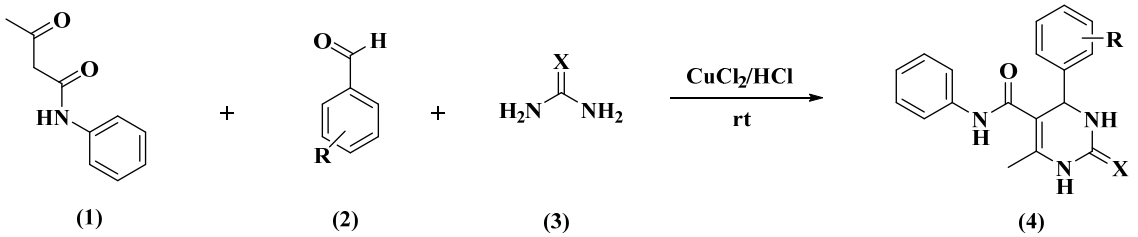

(1) (2) (3) (4)

Where, X = S and O
R= H, 4-OCH_3, 4-Me, 4-Cl, 4-Br

Figure 3.1

α-Keto acid **5** was incorporated into compounds **2** and **3** to yield 6-alkyl-5-carbonyl derivatives of the conventional Biginelli DHPM **6**. Compound **7** were acquired with a yield ranging from 22% to 100% when methanesulfonic acid served as the catalyst. Alongside the utilization of α-keto carboxylic acid **6**, monocarbonyl cyclic ketones **7** and **9** were likewise utilized in the three-component Biginelli-like reaction by the same authors. Aromatic ketones **7** and aliphatic ketones **9** underwent a three-component condensation to yield 5,6-dialkyl DHPMs **8**, **10a**, and **10b**, respectively (**Figure 3.2**).[91]

A variety of 3-(aryl)-1-phenyl-1*H*-pyrazole-4-carbaldehydes (**12**) with diverse electron-withdrawing and electron-releasing substituents, namely 4-F, 4-Cl, 4-Br, 4-NO_2 and 4-CH_3, were synthesized. All dihydropyrimidine derivatives (**13**) were produced via the multi-component Biginelli reaction, utilizing substituted aldehydes, ethyl or methyl acetoacetate, and urea derivatives.[92] A library including 30 dihydropyrimidines was produced and assessed for its in vitro antitubercular efficacy against mycobacterium tuberculosis H37Rv. Two chemicals, R = 4-fluorophenyl and R = 4-nitrophenyl **(14)** had the highest in vitro activity, with a minimum inhibitory concentration (MIC) of 0.02 µg/mL against Mycobacterium tuberculosis, surpassing the potency of isoniazid (**Figure 3.3**).[93]

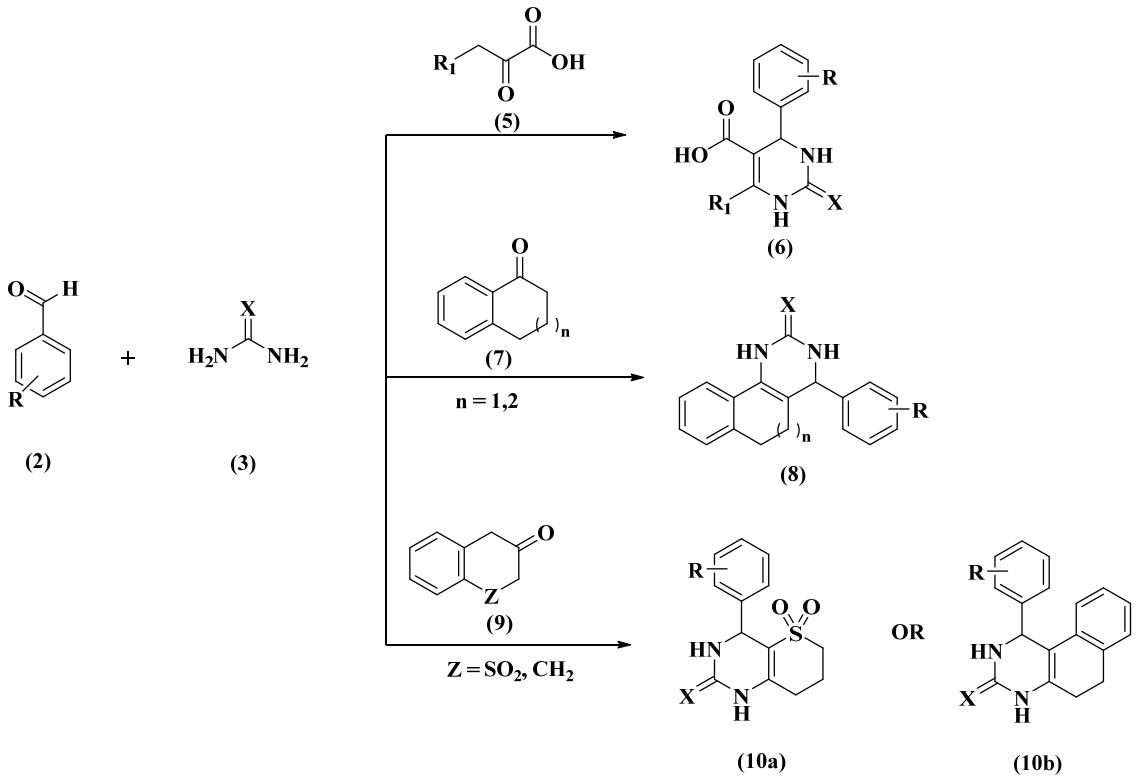
(2)
(3)
(5)
(6)
(7)
n = 1,2
(8)
(9)
Z = SO2, CH2
(10a)
OR
(10b)
Where, X = S and O
R= H, 4-OCH3, 4-Me, 4-Cl, 4-Br
R1= Ph, Me, 4-NO2Ph

Figure 3.2

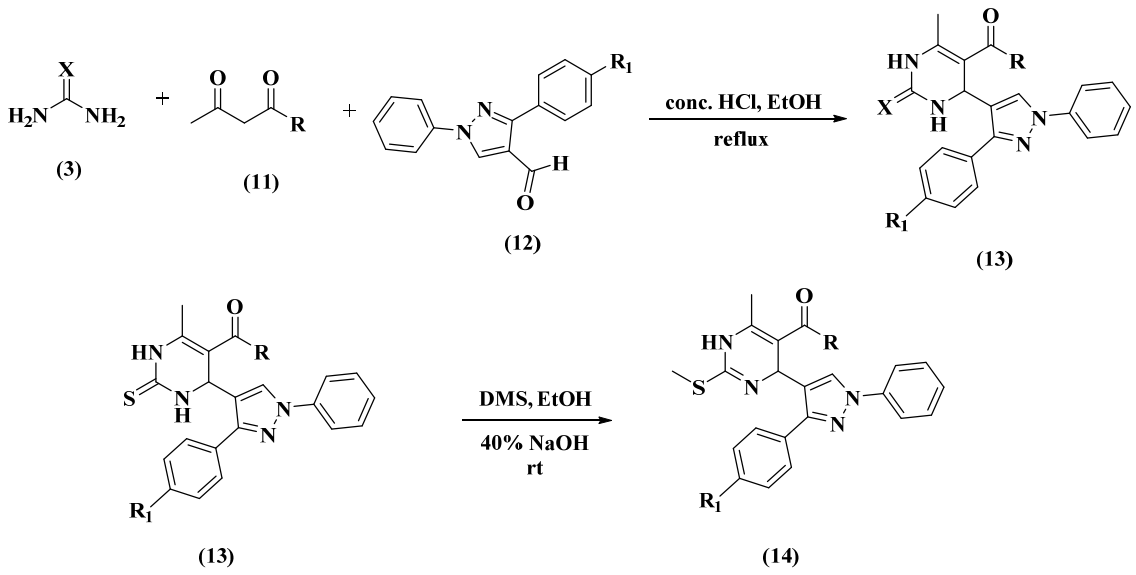
(3)
(11)
(12)
conc. HCl, EtOH
reflux
(13)
DMS, EtOH
40% NaOH
rt
(13)
(14)
Where, X = S and O
R= OCH3, OC2H5
R1= 4-F, 4-Cl, 4-Me, 4-NO2

Figure 3.3

Condensation in a single vessel of aldehyde **2**, ethyl trifluoro acetoacetate **15**, and thiourea **3** in a 1:1:1.5 ratio, conducted in refluxing THF for 24 h. The hexahydro pyrimidine **16**, regarded as an intermediate in the Biginelli reaction, was isolated in moderate to good yields (67–95%). Compound **16** react with p-toluene sulfonic acid in refluxing toluene to produce compound **17**. Further **17** was added into 2-bromo-1-(4-(trifluoromethyl)phenyl)ethan-1-one (**18**) and catalytic amount pyridine in refluxing ethanol for 3 h to produce target compound **19**. All derivatives were produced, and there in vitro cytotoxic effects were assessed in the colon cancer cell line (COLO 320 HSR). Compounds **16, 17** and **19** demonstrated the highest activity in this series (**Figure 3.4**).[94]

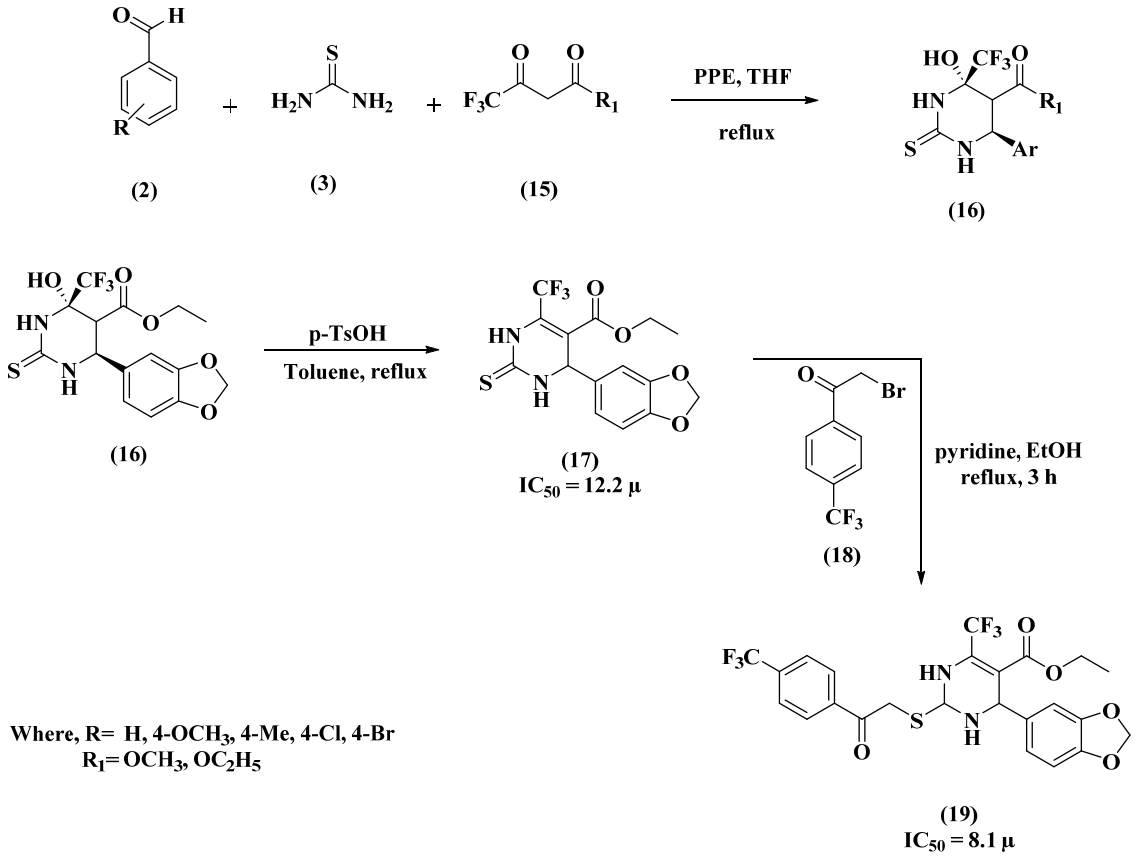

Figure 3.4

In 2014, Abranyi-Balogh et al. described 1-aryl-β-carboline-3-carbaldehydes **20** as adaptable building blocks, demonstrating their utility as starting materials for Biginelli-type reactions. Compound **20** was effectively reacted with urea **3** and compound **11**. The reaction

was catalyzed by $NiCl_2.6H_2O$ in ethanol with a catalytic quantity of concentrated HCl as solvent, yielding 2-oxo 1,2,3,4-tetrahydropyrimidine derivatives **21** in 36-90% yield (**Figure 3.5**).[95]

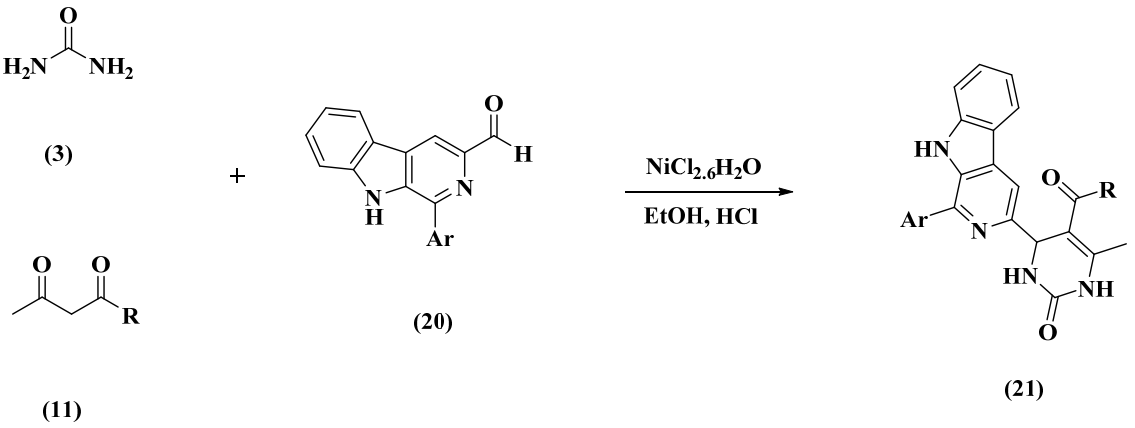

Figure 3.5

3.2 Results and Discussion

3.2.1 Chemistry

The synthetic route of quinoline containing DHPM hybrid molecules **(6a-j)** is depicted in Scheme 1. A combination of a suitable aromatic aldehyde **1**, thiourea **2** and ethyl acetoacetate **3** in methanol with 37% HCl was refluxed for 12 h, following which the reaction mixture was let to cool to yield compound **4**.[96] At last, compound **4** was treated with compound **5** (synthesised and depicted in chapter-1) with K_2CO_3 using acetone as a solvent at rt to yield the quinoline containing DHPM hybrid derivatives (**6a-j**).[97]

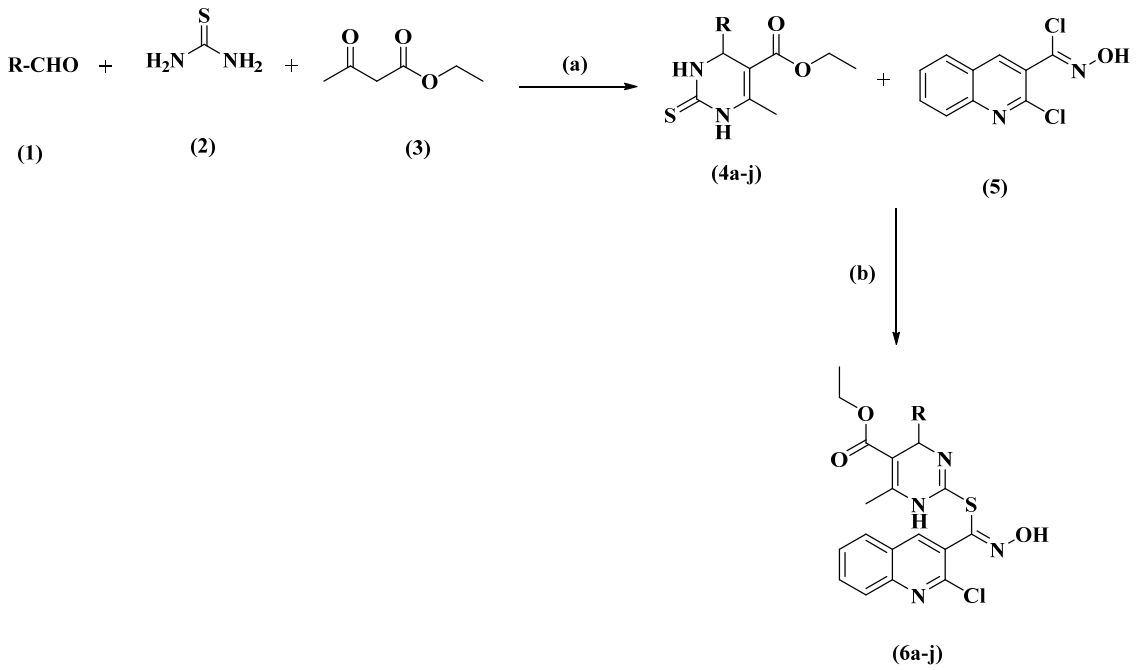

Reaction condition: a) Methanol, Conc. HCl, 80 °C, 12 h ; b) K_2CO_3, Acetone, rt, 2 h.

Scheme 1: Synthesis of the quinoline containing DHPM hybrid derivatives.

Table 1: Physicochemical characteristics of the novel quinoline containing DHPM hybrid derivatives (**6a-j**)

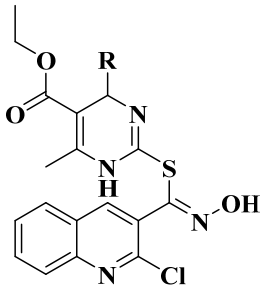

Compound	R	Molecular Weight	Molecular Formula	Yield (%)	Melting Point (°C)
6a	4-OCH_3-C_6H_4-	510.99	$C_{25}H_{23}ClN_4O_4S$	93	203-205
6b	4-Cl-C_6H_4-	515.41	$C_{24}H_{20}Cl_2N_4O_3S$	97	192-194
6c	1-C_4H_4S-	486.99	$C_{22}H_{19}ClN_4O_3S_2$	96	190-192
6d	4-CH_3-C_6H_4-	479.96	$C_{25}H_{23}ClN_4O_3S$	94	202-204
6e	3-Cl-C_6H_4-	515.41	$C_{24}H_{20}Cl_2N_4O_3S$	84	206-208

6f	4-OH-C_6H_4-	496.97	$C_{24}H_{21}ClN_4O_4S$	92	218-220
6g	2,5-OCH_3-C_6H_3-	541.02	$C_{26}H_{25}ClN_4O_5S$	90	215-217
6h	1-$C_{10}H_6ClN_2O$	566.46	$C_{27}H_{21}Cl_2N_5O_3S$	96	226-228
6i	4-F-C_6H_4-	498.96	$C_{24}H_{20}ClFN_4O_3S$	96	196-198
6j	C_6H_5-	480.97	$C_{24}H_{21}ClN_4O_3S$	99	198-200

3.3 Biological Activity

All newly synthesized hybrid quinoline derivatives with substituted DHPM (**6a–j**) were evaluated for their potential activity against two fungal strains: *Aspergillus niger* (ATCC 16888) and *Candida albicans* (ATCC 10231), two gram-positive bacteria: *Bacillus subtilis* (ATCC 6051) and *Staphylococcus aureus* (ATCC 23235), and two gram-negative bacteria: *Escherichia coli* (ATCC 25922) and *Salmonella typhi* (ATCC 19430). The inhibition zone (mm) was evaluated against ampicillin and gentamicin as positive controls for antibacterial activity, and nystatin as a positive control for antifungal activity. The test results indicate that the compounds had substantial activity against all bacterial and fungal species evaluated, with inhibition zones between 5 and 24 mm. The synthesized compounds exhibited moderate to superior inhibition compared to the reference medicines ampicillin, gentamicin, and nystatin. The antibacterial activity of the investigated substances was assessed using a concentration of 100 µg/ml in dimethyl sulfoxide (DMSO) as the solvent.

As shown in figures **1** & **2**, the antimicrobial evaluation revealed that these compounds exhibited significant bioactivity against most of the tested stains with an inhibition zone ranging from 5 to 24 mm.

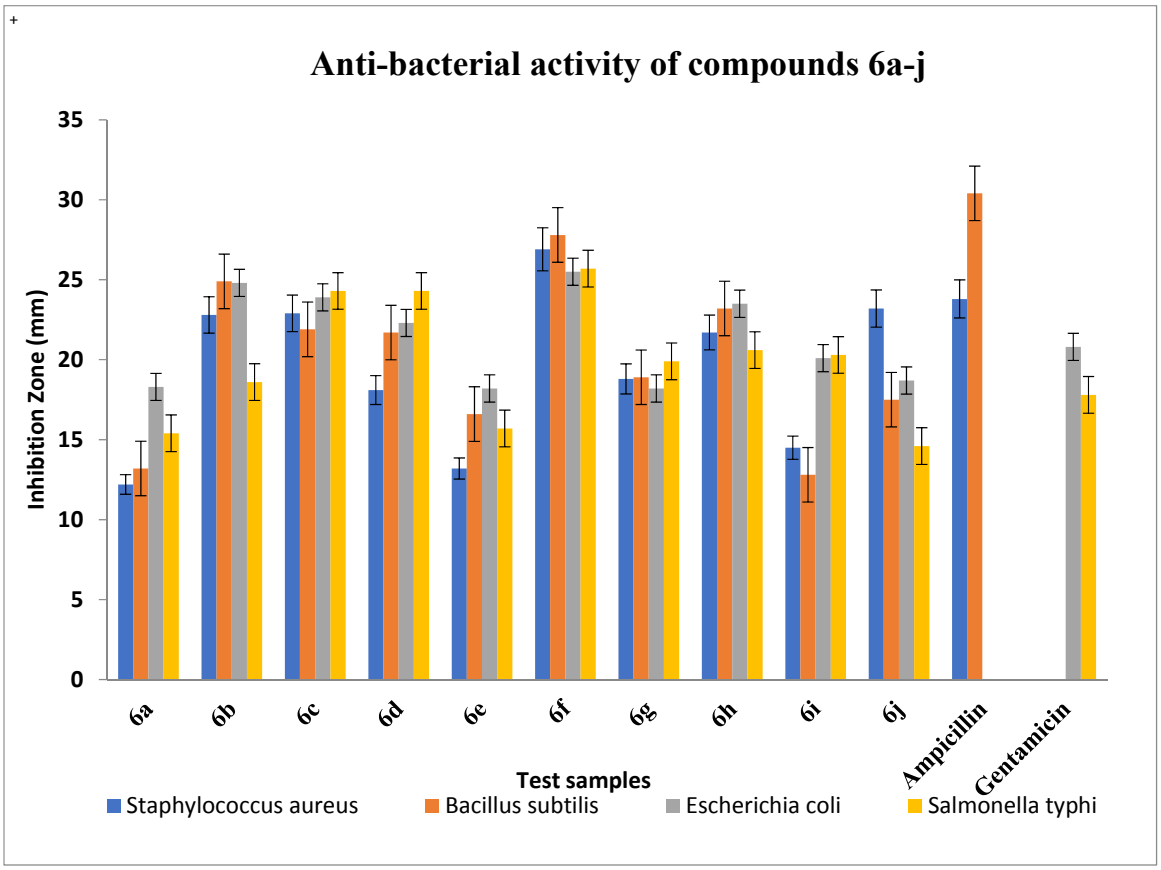

Figure 1: Graphical presentation of anti-bacterial activity of compounds **6a-j**.

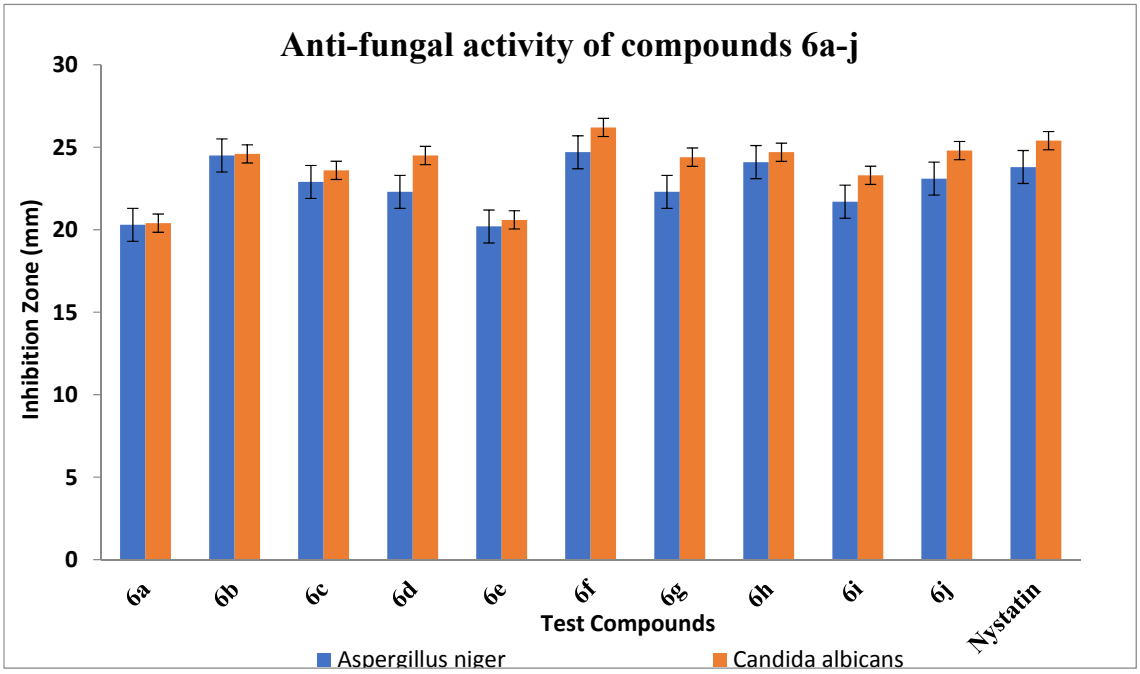

Figure 2: Graphical presentation of anti-fungal activity of compounds **6a-j**.

3.4 Structure-Activity Relationship (SAR):

Compound **6a** having methoxy substitution on the *para* position showed moderate antibacterial activity against *gram-negative* pathogens viz. *Escherichia coli* **(18.3 ± 1.1 mm**) and *Salmonella typhi* (**15.4 ± 0.34 mm**), while standard Gentamicin showed 20.8 ± 0.68 mm and 17.8 ± 0.33 mm against the respective pathogens. Compound **6b** having chloro substitution on the *para* position **(18.6 ± 0.42 mm)** and compound **6c (22.1 ± 0.33 mm)** having the presence of halogen group (Br) showed an increase in activity against *Salmonella typhi,* compared to compound **6a**. The inclusion of the electron donating group (CH_3) lies on the *para* position in compound **6d (24.3 mm)** showed good antimicrobial activity. The inclusion of the electron-withdrawing group (Cl) on the *ortho* position in compound **6e (15.7 mm)** showed decreased antibacterial activity against both *gram-negative* pathogens. Compound **6f** having hydroxy substitution on *para* position showed the most inhibition in antimicrobial activity **(27.8 ± 0.42 mm)** and also showed most inhibition in antifungal activity **(26.2 ± 0.42 mm)**. Dimethoxy group lies on *ortho* and *para* position in compound **6g** showed moderate anti-bacterial activity against *gram-negative* pathogens and moderate antifungal activity **(24.4mm)**. Compound **6f** having *p*-OH as a substitution exhibited moderate to high efficacy against all the pathogens.

3.5 Molecular Docking with *E. coli* DNA gyrase:

In silico investigations, particularly molecular modeling, are crucial for determining the potential binding mechanism of drugs with the target protein. A molecular docking study utilizing AutoDock Vina was conducted on the crystal structure of the 24 kDa domain of *E. coli* DNA gyrase, motivated by its biological relevance, potential as a drug target, availability of structural data, and the applicability of computational methods in drug discovery initiatives.[98] Subsequent to energy reduction, the produced three-dimensional molecular structures underwent docking analyses within the binding pocket of DNA gyrase. The docking study findings for synthesized hybrids **6a-j** are presented in Table **2**. Further, all prepared molecules exhibited good binding energy with the target varying from -6.8 to -8.3 $kJmol^{-1}$. Especially compound **6f** exhibited the highest docking score of –8.3 $kJmol^{-1}$ having three conventional hydrogen bonds with Arg A:20, Glu A:174 and Lys B:162.

Table 2. *In silico* docking results of the newly synthesized quinoline containing DHPM compounds **6a-j** and Gentamicin with the binding site of DNA gyrase.

Compounds	Docking score (kJ mol^{-1})	Interacting residues	Number of H-Bonds
6a	-6.8	Gln B: 135, Gln B:72	2
6b	-7.2	Lys B:162	1
6c	-7.6	Asp A:17,Glu B:58	2
6d	-71	Arg A:20	1
6e	-6.8	Arg B:204	1
6f	-8.3	Arg A:20, Glu A:174, Lys B:162	3
6g	-7.4	Lys B:162, Glu A:174, Arg A:20	3
6h	-7.8	Lys B:162, Glu B:58	2
6i	-7.5	Asp A:17, Lys B:162	2
6j	-7.0	Asp A:17, Lys B:162	2
Gentamicin	-6.9	Glu A:174, Arg A:20	2

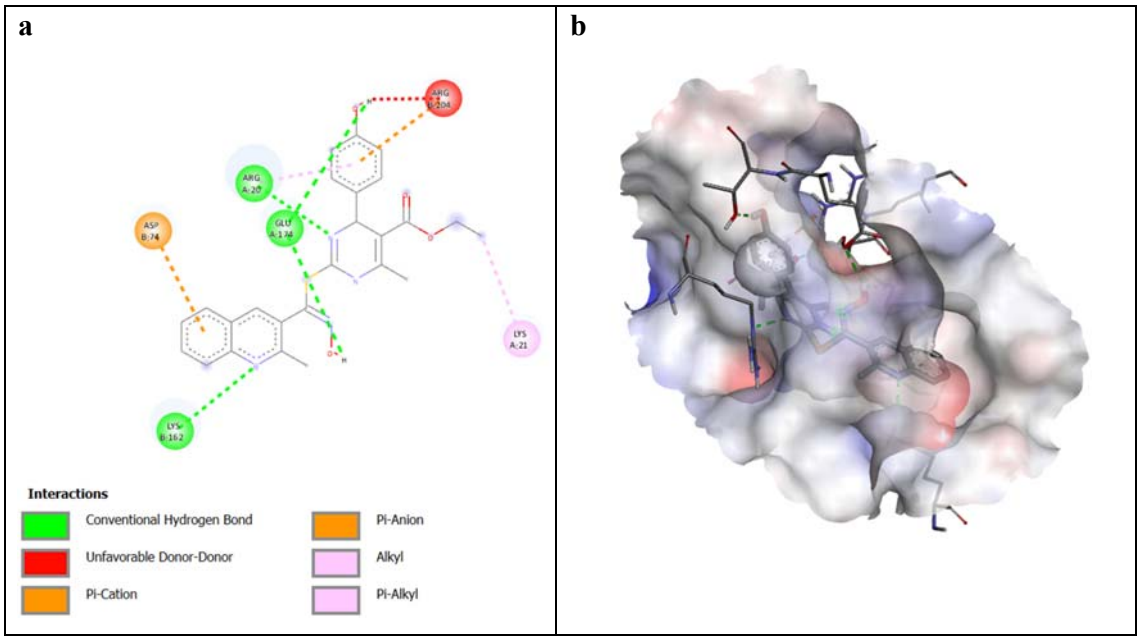

Figure 1. Docking pose of compound **6f** with 24 kDa domain of *E. coli* DNA gyrase. (**a**) Receptor-ligand interaction on a 2-D diagram, (**b**) Receptor-ligand interaction on a 3-D diagram.

The docking studies portrayed that for compound **6a** pyrimidine's amine formed H-bonding with Gln B: 135 and its -OH formed H-bindings with Gln B: 135. While in the case of compound **6b** the halogen atom formed H-bond with Lys B:162. In the case of compound **6c**, sulphur formed H-bond with Glu B:58 and -OH formed H-bindings with Asp A:17. In compound **6d** nitrogen atom of quinoline formed H-bonding with Arg A:20. In compound **6e** showed H-bonding with Arg B:204. Compound **6f** also interacted with three strong H-bonding with Arg A:20, Glu A:174 and Lys B:162, as displayed in (**Figure 1**), with the highest docking score of -8.3 kJ/mol, shown in (**Table 2**). Compound **6g** formed three conventional hydrogen bonds with Lys B:162, Glu A:174 and Arg A:20. Both compounds **6h** and **6i** showed two H-bonding with Asp A:17 and Lys B:162, out of which compound **6h** has a good docking score of -7.8 kJ mol^{-1} as mentioned in (**Table 2**). Compound **6j** also interacted with two H-bonding with Asp A:17, Lys B:162. Finally, the reference molecule gentamicin exhibited two robust hydrogen bonds with Arg A:20 and Glu A:174, as illustrated in (**Figure 2**), with a minimum docking score of -6.9 kJ mol-1 presented in (**Table 2**).

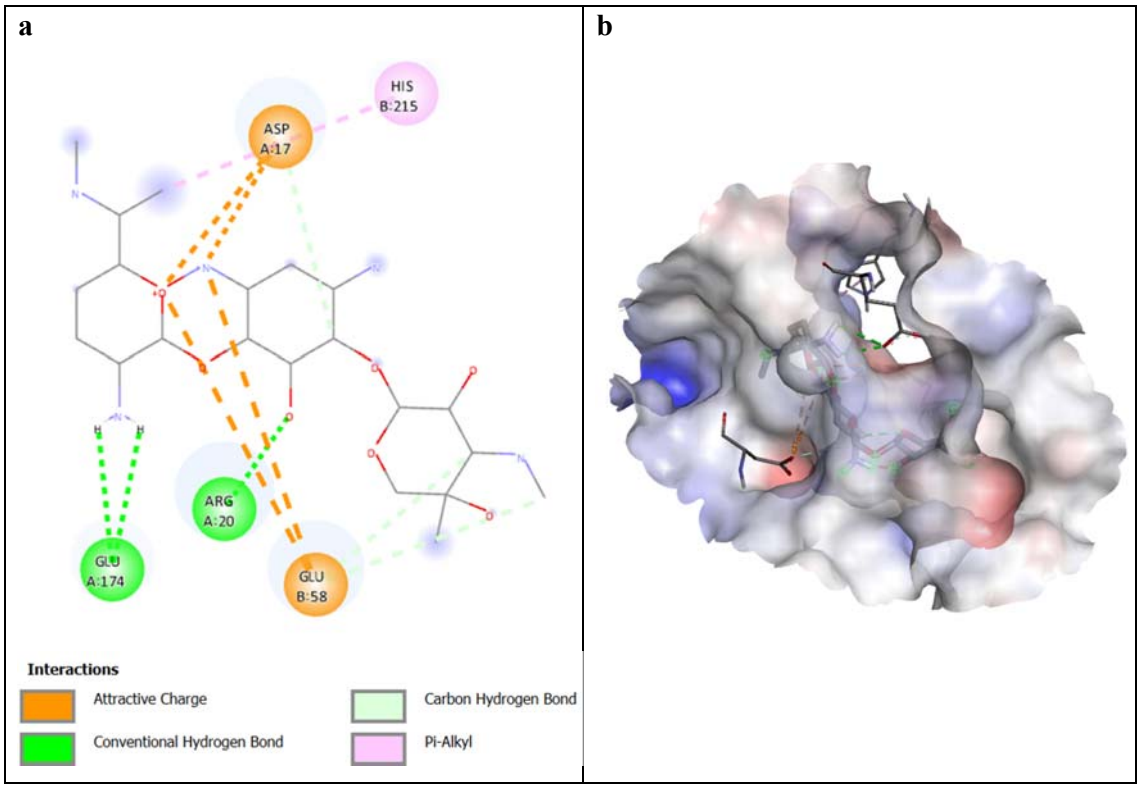

Figure 2. Docking pose of gentamicin with 24 kDa domain of *E. coli* DNA gyrase. (**a**) Receptor-ligand interaction on a 2-D diagram, (**b**) Receptor-ligand interaction on a 3-D diagram.

3.6 Conclusion:

A novel series of hybrid molecules of quinoline derivatives containing substituted DHPM was synthesized and characterized using NMR and Mass spectral analysis. All the synthesized molecules were evaluated for their antibacterial and antifungal properties. Most of the newly synthesized compounds showed excellent antibacterial efficacy against both pathogens. Out of all the synthesized compounds, compound **6f** showed promising results in antimicrobial activity with the highest docking score of -8.3 kJ/mol. While compounds **6d-f,** and **6h-i** were able to show good or moderate antibacterial and antifungal activity.

3.7 Experimental Section:

3.7.1 Chemistry

The open-capillary technique was employed to ascertain all melting points using an electrothermal apparatus (SUNTEK), and the results are unadjusted. Compounds were identified via thin-layer chromatography using UV light at 254 nm, 365 nm, and/or iodine vapor on precoated silica gel 60 F254 (Merck). A Bruker AVANCE III (400 MHz) spectrometer was employed to obtain ^{1}H and ^{13}C NMR spectra in DMSO-d_6, and $CDCl_3$, utilizing tetramethyl silane (TMS) as an internal standard, with chemical shifts expressed in ppm. The Shimadzu GCMS QP2010 Ultra mass spectrometer was employed to acquire mass spectra using a direct intake probe. All reagents acquired from Sigma-Aldrich, Spectrochem, and TCI were utilized without additional purification.

General procedure for the synthesis of compound (4a-j):[96]

A round-bottomed flask fitted with a spin vane and reflux condenser was charged with substituted aldehydes (**1**, 1 mmol), urea (**2**, 1 mmol), ethyl acetoacetate (**3**, 1 mmol) and 0.5 mL of 95% ethanol. A 7 to 8 drop of concentrated HCl was introduced to the mixture, and the system was subjected to reflux for 12 hours. The reaction flask was cooled to 0 °C, and the resulting precipitate was recovered by filtering and rinsed with lukewarm ethanol, the precipitate that was produced was then dried and recrystallized from ethanol in order to obtain the target molecule (**4a-j**), which are sufficiently pure to use in the next step.

Table 2: Physicochemical characteristics of the DHPM derivatives (**4a-j**).

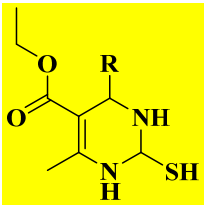

Compound	R	Molecular Weight	Molecular Formula	Yield (%)	Melting Point (°C)
4a	4-OCH_3-C_6H_4-	306.38	$C_{15}H_{18}N_2O_3S$	88	179-181[96]
4b	4-Cl-C_6H_4-	310.80	$C_{14}H_{15}ClN_2O_3S$	86	201-203[99]
4c	1-C_4H_4S-	282.38	$C_{12}H_{14}N_2O_2S_2$	82	132-134[100]
4d	4-CH_3-C_6H_4-	290.38	$C_{15}H_{18}N_2O_2S$	88	192-194[101]
4e	3-Cl-C_6H_4-	310.80	$C_{14}H_{15}ClN_2O_3S$	83	199-201[102]
4f	4-OH-C_6H_4-	292.35	$C_{14}H_{16}N_2O_3S$	80	193-195[103]
4g	2,5-OCH_3-C_6H_3-	336.41	$C_{16}H_{20}N_2O_4S$	94	203-205[104]
4h	1-$C_{10}H_6ClN_2O$	361.84	$C_{17}H_{16}ClN_3O_2S$	92	271-273[105]
4i	4-F-C_6H_4-	294.34	$C_{14}H_{15}FN_2O_3S$	94	191-193[106]
4j	C_6H_5-	276.35	$C_{14}H_{16}N_2O_2S$	86	197-199[96]

General procedure for the synthesis of compounds (6a-j):

To a well stirred solution of compound **4** (1 mmol) in an acetone (10 mL), (*Z*)-2-chloro-*N*-hydroxyquinoline-3-carbimidoyl chloride (**5**, 1 mmol) and K_2CO_3 (2 mmol) were added, and the mixture was stirred at rt for 2 h, after completion of the reaction (monitored by TLC), the reaction mixture was poured onto ice cold water and the formed precipitate was collected by filtration with suction, washed with water, and dried. The obtained residue was slurry washed with diethyl ether to give the title compound which are analytically pure.

By using the same general synthetic procedure for **6a-j**, the following compounds were prepared:

Ethyl (*Z*)-2-(((2-chloroquinolin-3-yl)(hydroxyimino)methyl)thio)-4-(4-methoxyphenyl)-6-methyl-1,4-dihydropyrimidine-5-carboxylate (6a):

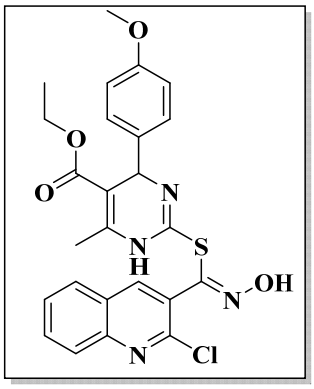

Compound **6a** was prepared from **4a** (0.25 g, 0.83 mmol), **5** (0.20 gm, 0.83 mmol) and K_2CO_3 (0.24 gm, 1.66 mmol) in acetone. An off-white solid (93% yield); mp: 203-205 °C. ^{1}H NMR (400 MHz, DMSO) δppm: 10.79 (s, OH), 9.90 (s, Ar-NH), 9.19 (s, Ar-H), 8.24 (d, *J* = 8.0 Hz, 1H, Ar-H), 8.04 (d, *J* = 8.4 Hz, 1H, Ar-H), 7.95 (t, *J* = 1.4 Hz, 1H, Ar-H), 7.68-7.63 (m, 3H, 3 × Ar-H), 7.02 (d, *J* = 9.2 Hz, 2H, 2 ×Ar-H), 5.00 (s, Ar-H), 4.52 (q, *J* = 7.3 Hz, 2H, CH_2), 3.47 (s, 3H, OCH_3), 2.29 (s, 3H, CH_3), 1.18 (t, *J* = 7.2 Hz, 3H, CH_3). ^{13}C NMR (101 MHz, $CDCl_3$) δppm: 189.30, 181.70, 165.13, 154.54, 154.31, 147.61, 133.63, 133.44, 132.05, 129.72, 127.74, 125.05, 124.63, 119.30, 114.38, 110.66, 59.27, 55.26, 20.001, 10.001. Mass spectrum: 511 *m/z* (M^+).

Ethyl (*Z*)-4-(4-chlorophenyl)-2-(((2-chloroquinolin-3-yl)(hydroxyimino)methyl)thio)-6-methyl-1,4-dihydropyrimidine-5-carboxylate (6b):

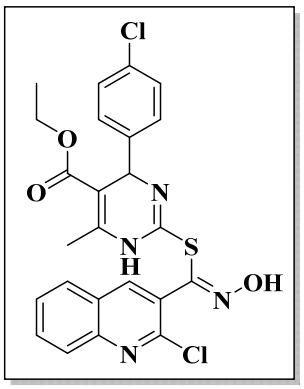

Compound **6b** was prepared from **4b** (0.26 g, 0.83 mmol), **5** (0.20 gm, 0.83 mmol) and K_2CO_3 (0.23 gm, 1.66 mmol) in acetone. An off-white solid (0.18 g, 97% yield); mp: 192-194 °C. ^{1}H NMR (400 MHz, DMSO) δppm: 9.24 (s, 1H, OH), 8.64 (s, 1H, Ar-NH), 8.03 (s, 1H, Ar-H),

8.00 (d, *J* = 13.3 Hz, 1H, Ar-H), 7.96 – 7.82 (m, 1H, Ar-H), 7.73 (dd, *J* = 15.5, 8.0 Hz, 2H, 2 ×Ar-H), 7.39 (d, *J* = 8.5 Hz, 2H, 2 ×Ar-H), 7.25 (d, *J* = 8.5 Hz, 2H, 2 ×Ar-H), 5.14 (d, *J* = 3.4 Hz, 1H, Ar-H), 3.99 (q, *J* = 7.0 Hz, 2H, CH_2), 2.25 (s, 3H, CH_3), 1.10 (t, *J* = 7.1 Hz, 3H, CH_3). ^{13}C NMR (101 MHz, DMSO) δppm: 165.67, 152.40, 149.21, 145.05, 144.26, 139.31, 134.83, 132.24, 132.05, 128.92, 128.87, 128.66, 128.42, 128.30, 127.95, 127.25, 123.69, 99.28, 59.73, 53.87, 18.28, 14.54. Mass spectrum: 515 *m/z* (M^+).

Ethyl (*Z*)-2-(((2-chloroquinolin-3-yl)(hydroxyimino)methyl)thio)-6-methyl-4-(thiophen-2-yl)-1,4-dihydropyrimidine-5-carboxylate (6c):

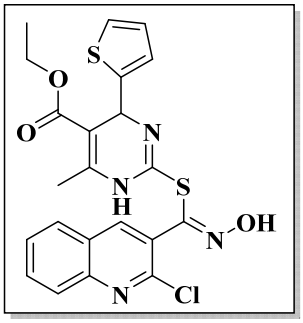

Compound **6c** was prepared from **4c** (0.21 g, 0.83 mmol), **5** (0.20 gm, 0.83 mmol) and K_2CO_3 (0.23 gm, 1.66 mmol) in acetone. An off-white solid (0.19 g, 96% yield); mp: 190-192 °C. ^{1}H NMR (400 MHz, DMSO) δppm: 9.30 (s, 1H, OH), 8.57 (s, 1H, Ar-NH), 7.98 (dd, *J* = 13.4, 8.3 Hz, 2H, 2 × Ar-H), 7.91 (s, 1H, Ar-H), 7.84 (t, *J* = 7.7 Hz, 1H, Ar-H), 7.70 (t, *J* = 7.7 Hz, 1H, Ar-H), 7.37 (dd, *J* = 19.6, 4.9 Hz, 1H, Ar-H), 6.95 (d, *J* = 8.6 Hz, 1H, Ar-H), 6.89 (d, *J* = 3.6 Hz, 1H, Ar-H), 5.42 (d, *J* = 3.8 Hz, 1H, Ar-H), 4.05 (q, *J* = 7.0 Hz, 2H, CH_2), 2.21 (s, 3H, CH_3), 1.16 (t, *J* = 7.1 Hz, 3H, CH_3).^{13}C NMR (101 MHz, DMSO) δppm: 165.52, 152.75, 149.18, 149.10, 146.63, 145.00, 134.69, 132.04, 128.89, 128.39, 128.31, 128.24, 127.17, 126.71, 125.10, 124.68, 124.01, 123.64, 100.30, 60.26, 49.79, 18.13, 14.60. Mass spectrum: 487 *m/z* (M^+).

Ethyl (*Z*)-2-(((2-chloroquinolin-3-yl)(hydroxyimino)methyl)thio)-6-methyl-4-(*p*-tolyl)-1,4-dihydropyrimidine-5-carboxylate (6d):

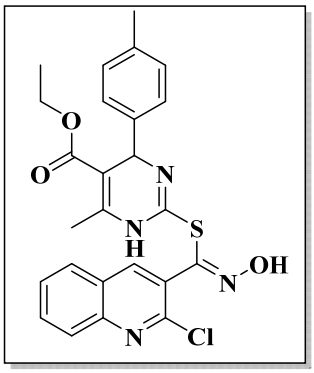

Compound **6d** was prepared from **4d** (0.24 g, 0.83 mmol), **5** (0.20 gm, 0.83 mmol) and K_2CO_3 (0.23 gm, 1.66 mmol) in acetone. An off-white solid (0.17 g, 94% yield); mp: 202-204 °C. ^{1}H NMR (400 MHz, $CDCl_3$) δppm: 8.52 (s, 1H, Ar-H), 8.07 (d, *J* = 8.5 Hz, 1H, Ar-H), 7.97 (d, *J* = 8.2 Hz, 1H, Ar-H), 7.93 (t, *J* = 7.7 Hz, 1H, Ar-H), 7.73 (t, *J* = 7.6 Hz, 1H, Ar-H), 7.33 (d, *J* = 8.3 Hz, 2H, 2 × Ar-H), 7.17 (d, *J* = 8.3 Hz, 2H, 2 × Ar-H), 5.06 (s, Ar-H), 4.24 (q, 1.45 Hz, 2H, CH_2), 2.20 (s, 6H, 2 × CH_3), 1.13 (t, *J* = 8.0 Hz, 3H, CH_3). ^{13}C NMR (101 MHz, DMSO) δppm: 188.58, 163.26, 163.09, 162.54, 160.53, 156.25, 148.58, 137.95, 135.70, 133.95, 132.08, 129.46, 126.53, 122.42, 121.85, 119.79, 117.87, 114.30, 61.47, 20.97, 18.45, 16.22. Mass spectrum: 495 *m/z* (M^+).

Ethyl (*Z*)-4-(3-chlorophenyl)-2-(((2-chloroquinolin-3-yl)(hydroxyimino)methyl)thio)-6-methyl-1,4-dihydropyrimidine-5-carboxylate (6e):

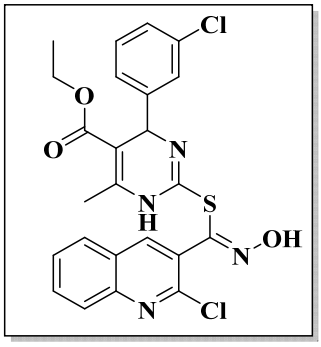

Compound **6e** was prepared from **4e** (0.26 g, 0.83 mmol), **5** (0.20 gm, 0.83 mmol) and K_2CO_3 (0.23 gm, 1.66 mmol) in acetone. An off-white solid (0.17 g, 94% yield); mp: 206-208 °C. ^{1}H NMR (400 MHz, $CDCl_3$) δppm: 8.53 (s, 1H, Ar-H), 8.08 (d, *J* = 8.5 Hz, 1H, Ar-H), 7.99 (d, *J* = 8.2 Hz, 1H, Ar-H), 7.93 (t, *J* = 7.7 Hz, 1H, Ar-H), 7.74 (t, *J* = 7.6 Hz, 1H, Ar-H), 7.39 – 7.24

(m, 3H, 3 × Ar-H), 7.06 (d, *J* = 8.0 Hz, 1H, Ar-H), 5.06 (s, 1H, Ar-H), 4.17 (q, 7.4 Hz, 2H, CH_2), 2.23 (s, 3H, CH_3), 1.24 (t, *J* = 8.0 Hz, 3H, CH_3). ^{13}C NMR (101 MHz, DMSO) δppm: 184.97, 163.26, 163.08, 162.68, 160.86, 148.47, 138.10, 135.97, 135.72, 135.31, 133.93, 129.46, 128.28, 127.42, 125.96, 121.84, 120.02, 117.90, 61.46, 20.97, 18.69, 18.46, 16.13. Mass spectrum: 516 *m/z* (M^+).

Ethyl (*Z*)-2-(((2-chloroquinolin-3-yl)(hydroxyimino)methyl)thio)-4-(4-hydroxyphenyl)-6-methyl-1,4-dihydropyrimidine-5-carboxylate (6f):

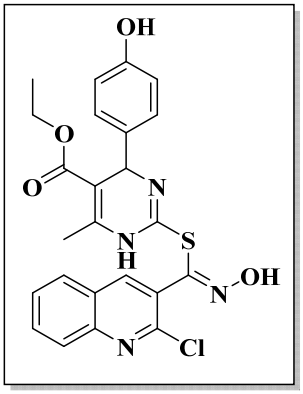

Compound **6f** was prepared from **4f** (0.24 g, 0.83 mmol), **5** (0.20 gm, 0.83 mmol) and K_2CO_3 (0.23 gm, 1.66 mmol) in acetone. An off-white solid (0.16 g, 92% yield); mp: 218-220 °C. ^1H NMR (400 MHz, DMSO) δppm: 9.34 (s, 1H, OH), 9.12 (s, 1H, Ar-NH), 8.07 – 7.39 (m, 7H, 7 × Ar-H), 7.03 (d, *J* = 8.2 Hz, 2H, 2 × Ar-H), 6.69 (d, *J* = 8.2 Hz, 2H, 2 × Ar-H), 5.04 (s, 1H Ar-H), 4.01 (q, *J* = 7.1 Hz, 2H, CH_2), 2.23 (s, 3H, CH_3), 1.10 (t, *J* = 7.1 Hz, 3H, CH_3). ^{13}C NMR (101 MHz, DMSO) δppm: 191.51, 163.29, 162.92, 160.53, 158.04, 156.26, 148.51, 137.91, 134.58, 132.07, 126.65, 123.97, 123.90, 122.43, 119.93, 117.82, 115.79, 115.57, 114.30, 61.48, 16.22, 14.47. Mass spectrum: 497 *m/z* (M^+).

Ethyl (*Z*)-2-(((2-chloroquinolin-3-yl)(hydroxyimino)methyl)thio)-4-(2,5-dimethoxy-phenyl)-6-methyl-1,4-dihydropyrimidine-5-carboxylate (6g):

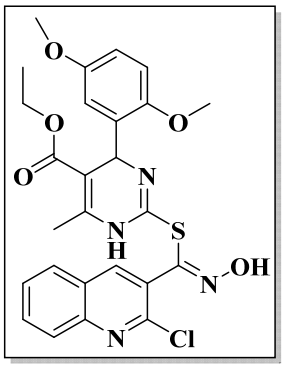

Compound **6g** was prepared from **4g** (0.28 g, 0.83 mmol), **5** (0.20 gm, 0.83 mmol) and K_2CO_3 (0.23 gm, 1.66 mmol) in acetone. An off-white solid (0.15 g, 90% yield); mp: 215-217 °C. ^{1}H NMR (400 MHz, DMSO) δppm: 9.13 (s, 1H, OH), 8.64 (s, 1H, Ar-NH), 8.01 (d, *J* = 12.4 Hz, 2H, 2 × Ar-H), 7.86 (d, *J* = 8.4 Hz, 1H, Ar-H), 7.73 (t, *J* = 7.6 Hz, 1H, Ar-H), 7.27 (t, *J* = 2.7 Hz, 1H, Ar-H), 6.92 (d, *J* = 8.9 Hz, 1H, Ar-H), 6.80 (d, *J* = 8.8 Hz, 1H, Ar-H), 6.59 (d, *J* = 3.1 Hz, 1H, Ar-H), 5.44 (s, 1H, Ar-H), 3.93 (q, *J* = 7.1 Hz, 2H, CH_2), 3.74 (s, 3H, OCH_3), 3.66 (s, 3H, OCH_3), 2.28 (s, 3H, CH_3), 1.04 (t, *J* = 7.1 Hz, 3H, CH_3). ^{13}C NMR (101 MHz, DMSO) δppm: 165.77, 153.35, 152.59, 151.19, 149.31, 146.63, 145.05, 139.31, 134.83, 133.30, 132.06, 128.92, 128.42, 128.30, 127.25, 123.69, 114.51, 112.61, 112.43, 98.01, 59.48, 56.37, 55.73, 49.57, 18.15, 14.51. Mass spectrum: 541 *m/z* (M^+).

Ethyl (*Z*)-4-(2-chloroquinolin-3-yl)-2-(((2-chloroquinolin-3-yl)(hydroxyimino)methyl)-thio)-6-methyl-1,4-dihydropyrimidine-5-carboxylate (6h):

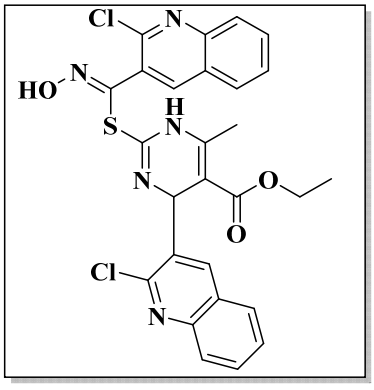

Compound **6h** was prepared from **4h** (0.21 g, 0.83 mmol), **5** (0.20 gm, 0.83 mmol) and K_2CO_3 (0.23 gm, 1.66 mmol) in acetone. An yellow solid (0.18 g, 96% yield); mp: 226-228 °C. Mass spectrum: 541 *m/z* (M^+).

Ethyl (*Z*)-2-(((2-chloroquinolin-3-yl)(hydroxyimino)methyl)thio)-4-(4-fluorophenyl)-6-methyl-1,4-dihydropyrimidine-5-carboxylate (6i):

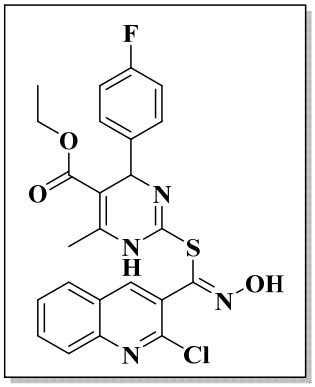

Compound **6i** was prepared from **4i** (0.26 g, 0.83 mmol), **5** (0.20 gm, 0.83 mmol) and K_2CO_3 (0.23 gm, 1.66 mmol) in acetone. An off-white solid (0.18 g, 96% yield); mp: 196-198 °C. ^{1}H NMR (400 MHz, DMSO) δppm: 10.37 (s, 1H, OH), 9.66 (s, 1H, NH), 8.66 (s, 1H, Ar-H), 8.02 (dd, *J* = 12.9, 8.3 Hz, 2H, 2 × Ar-H), 7.87 (t, *J* = 6.9 Hz, 1H, Ar-H), 7.73 (t, *J* = 7.5 Hz, 1H, Ar-H), 7.30 – 7.11 (m, 4H, 4 ×Ar-H), 5.16 (s, 1H, Ar-H), 4.07 – 3.94 (m, 2H, CH_2), 2.30 (s, 3H, CH_3), 1.10 (td, *J* = 7.1, 3.3 Hz, 3H, CH_3). ^{13}C NMR (101 MHz, $CDCl_3$) δ 174.64, 165.13, 152.82, 147.56, 145.99, 145.16, 142.77, 138.36, 132.37, 130.97, 128.59, 128.54, 128.21, 127.17, 126.91, 124.65, 115.91, 115.70, 102.91, 60.53, 55.56, 18.41, 14.13. Mass spectrum: 499 *m/z* (M^+).

Ethyl (*Z*)-2-(((2-chloroquinolin-3-yl)(hydroxyimino)methyl)thio)-6-methyl-4-phenyl-1,4-dihydropyrimidine-5-carboxylate (6j):

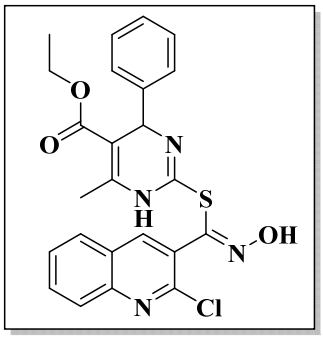

Compound **6j** was prepared from **4j** (0.27 g, 0.83 mmol), **5** (0.20 gm, 0.83 mmol) and K_2CO_3 (0.23 gm, 1.66 mmol) in acetone. An off-white solid (0.18 g, 98% yield); mp: 198-200 °C. ^{1}H NMR (400 MHz, DMSO) δppm: 9.20 (s, 1H, OH), 8.65 (s, 1H, Ar-NH), 8.07 – 7.97 (m, 2H, 2 × Ar-H), 7.87 (t, *J* = 8.4, 6.9, 1.5 Hz, 1H, Ar-H), 7.73 (ddd, *J* = 8.1, 5.4, 1.3 Hz, 2H, 2 × Ar-H), 7.38 – 7.29 (m, 2H, 2 × Ar-H), 7.29 – 7.19 (m, 3H, 3 × Ar-H), 5.14 (d, *J* = 3.4 Hz, 1H, Ar-H), 3.98 (q, *J* = 7.0 Hz, 2H, CH_2), 2.25 (s, 3H, CH_3), 1.10 (t, *J* = 7.1 Hz, 3H, CH_3). ^{13}C NMR (101 MHz, DMSO) δppm: 165.80, 152.59, 148.84, 146.63, 145.34, 145.06, 139.31, 134.85, 132.07, 128.93, 128.86, 128.42, 128.30, 127.74, 127.26, 126.72, 123.70, 99.70, 59.65, 54.42, 18.25, 14.55.

3.7.2 Experiment protocol of anti-microbial activity

The antibacterial and antifungal efficacy was evaluated against the prevalent fungal pathogens *Aspergillus niger and Candida albicans*, as well as two gram-positive bacterial strains (*Bacillus subtilis and Staphylococcus aureus*) and two gram-negative bacterial strains (*Escherichia coli and Salmonella typhi*). The antibacterial and antifungal standards utilized to assess the inhibition zone (mm) were Ampicillin (100 µg/ml), Gentamicin (100 µg/ml), and Nystatin (100 µg/ml), respectively. The experimental results indicated that all bacterial strains were significantly inhibited by the investigated substances, exhibiting inhibition zones between 15 and 33 mm, whereas fungal species had inhibition zones ranging from 13 to 32 mm. The synthesized molecule exhibited enhanced and moderate efficacy relative to reference medications. The antibacterial activity of the investigated chemical was assessed using a concentration of 100 µg/ml of the molecule in the solvent DMSO. Figures **2** and **3** offer a graphical depiction of the antibacterial activity data.[107]

3.7.3 Experiment protocol of molecular docking study

The ChemSketch 2021.2.0 program facilitated the creation of ligand structures. Additionally, docking experiments were conducted to identify the interaction residues of all drugs. AutoDock Vina 1.1.2 was utilized, and during the docking study, the energy minimization of each molecule was conducted using Avogadro-1.2.0. The crystal structure of the 24 kDa domain of *E. coli* DNA gyrase was obtained from the PDB database (4DUH).[108] The structural receptor was free of all ligands prior to docking by excluding heteroatoms. Kollaman charge, solvation

parameters, and polar hydrogens were incorporated into the protein to finalize its processing. The designated grid box dimensions for x, y, and z were established at 40 Å, 40 Å, and 40 Å, respectively. The grid centre for the variables x, y, and z was established at 29.712, 2.093, and 23.925, respectively. The exhaustiveness was 40, and the grid point spacing was 0.375 Å. The probable binding mechanism was ascertained utilizing the advanced molecular graphics viewer Discovery Studio Visualizer v21.0.[109]

3.8 Spectral data

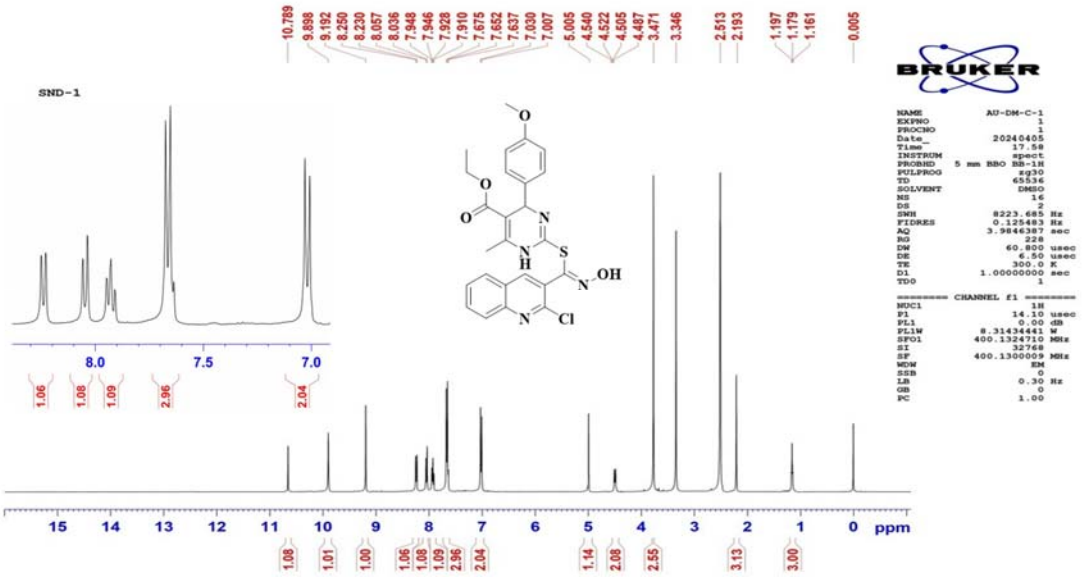

Figure 1: ^{1}H NMR of compound **6a**

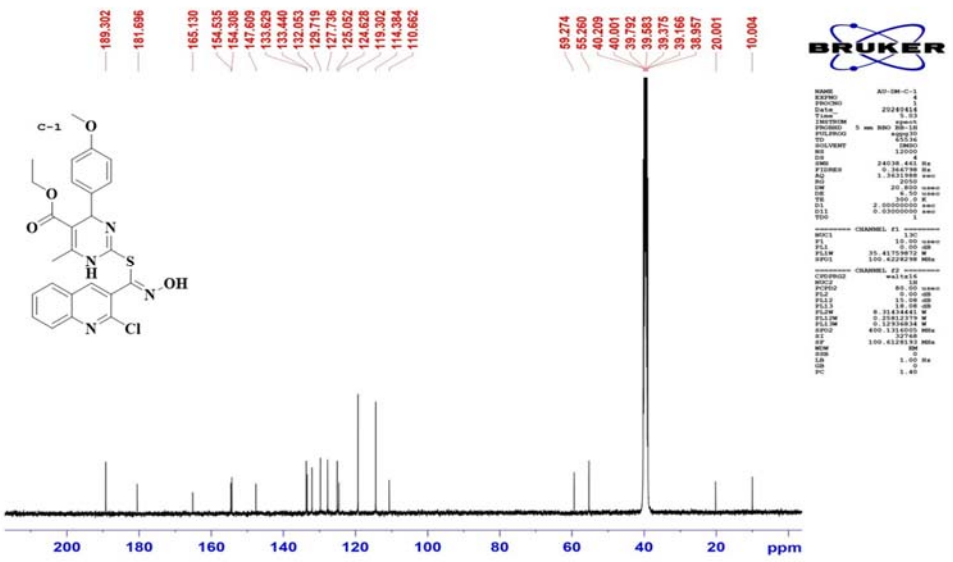

Figure 2: ^{13}C NMR of compound **6a**

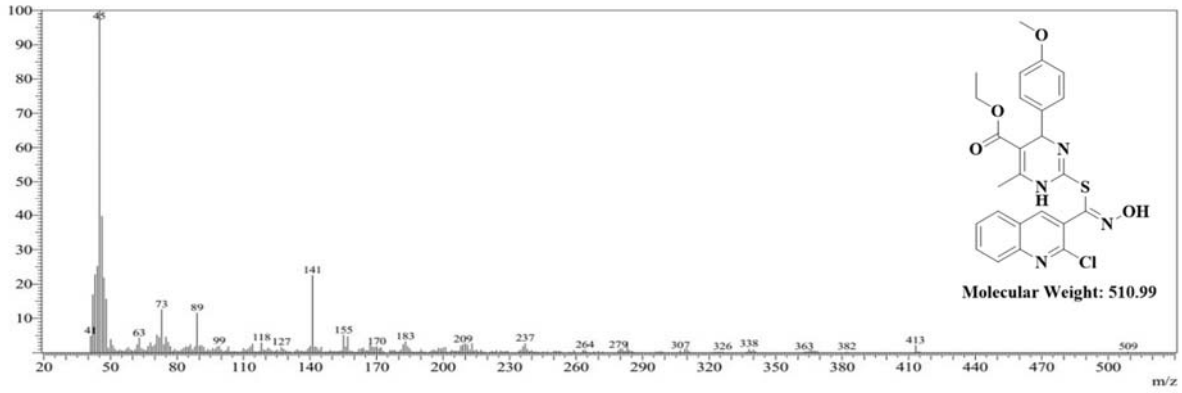

Figure 3: Mass spectrum of compound **6a**

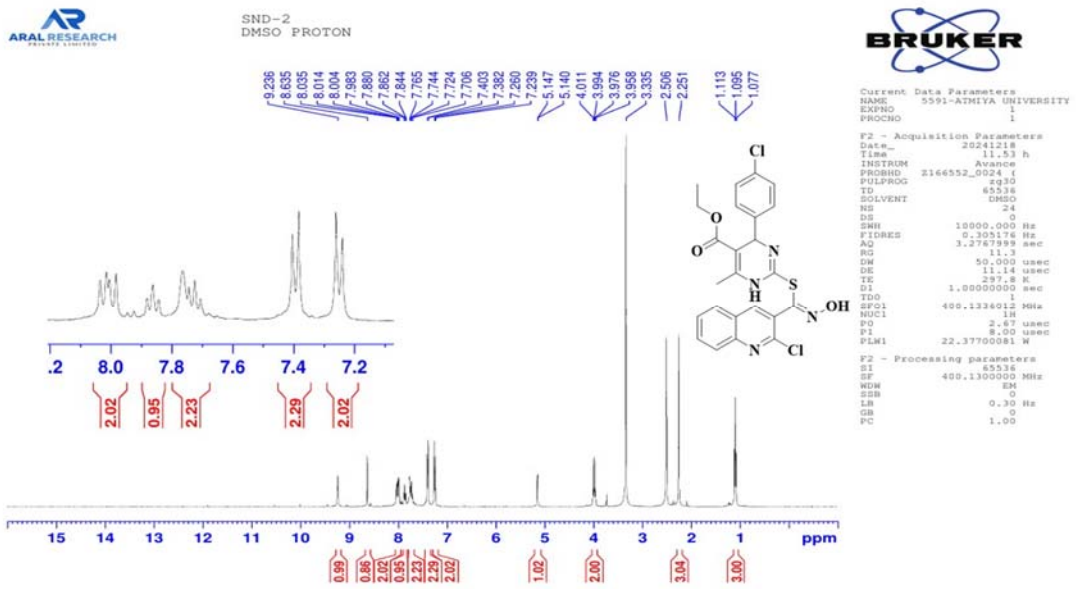

Figure 4: ^{1}H NMR of compound **6b**

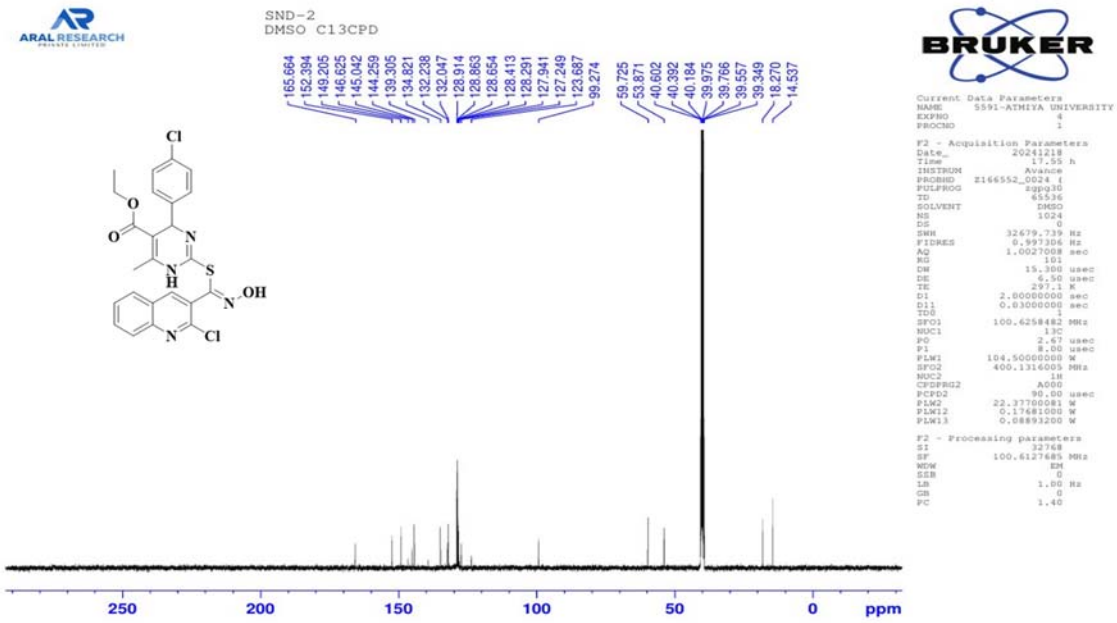

Figure 5: ^{13}C NMR of compound **6b**

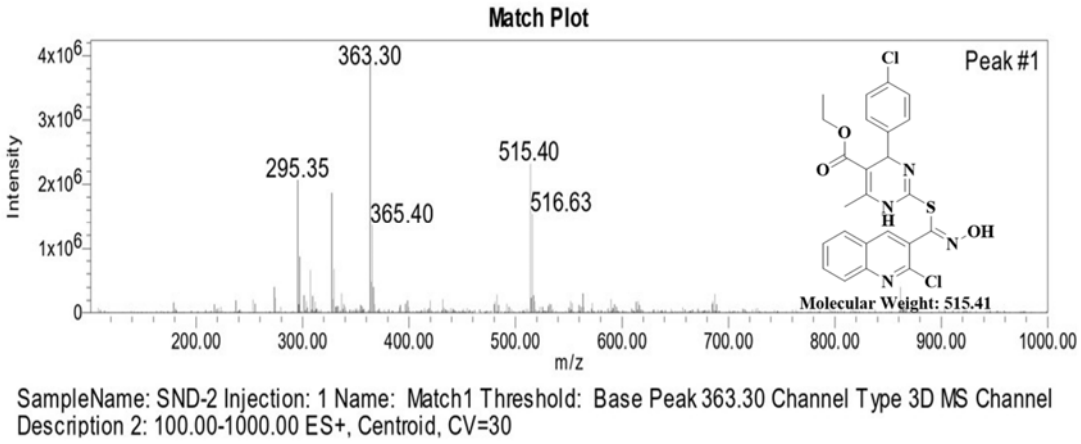

Figure 6: Mass spectrum of compound **6b**

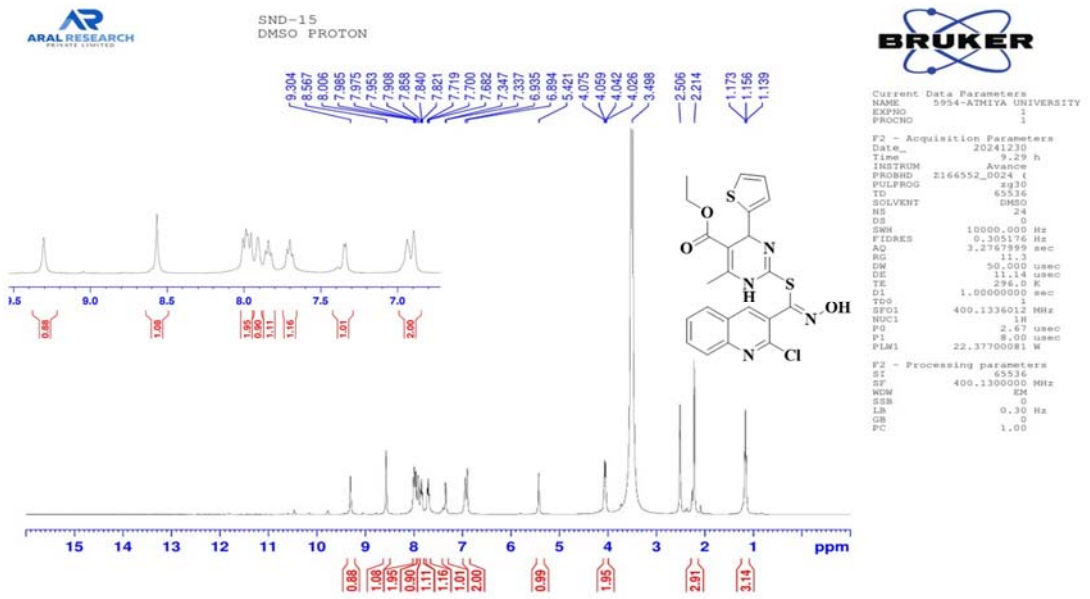

Figure 7: ^{1}H NMR of compound **6c**

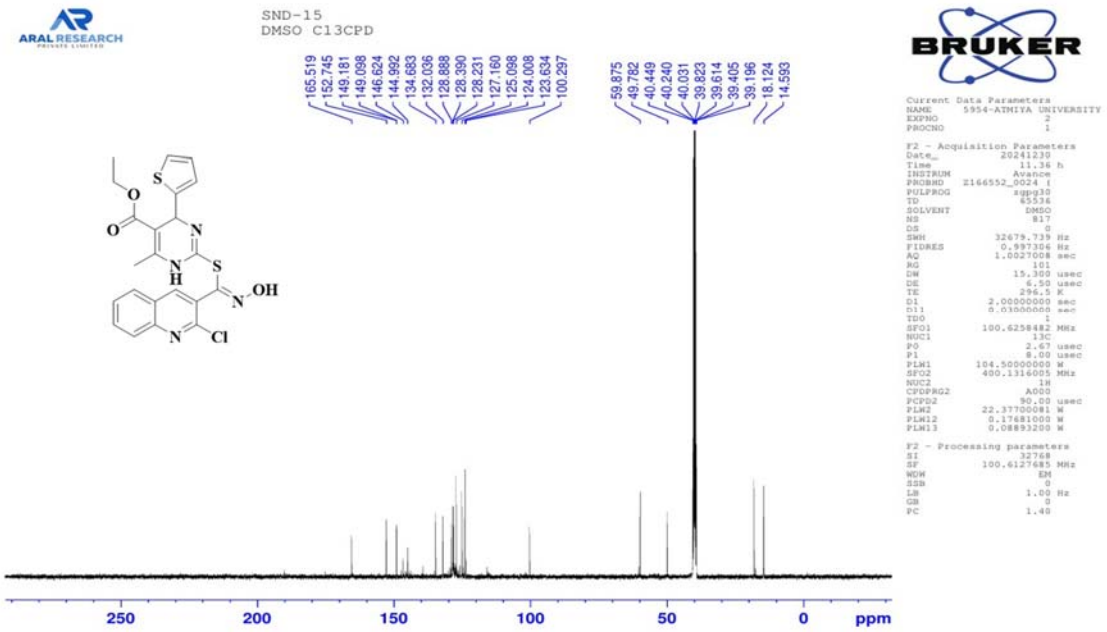

Figure 8: ^{13}C NMR of compound **6c**

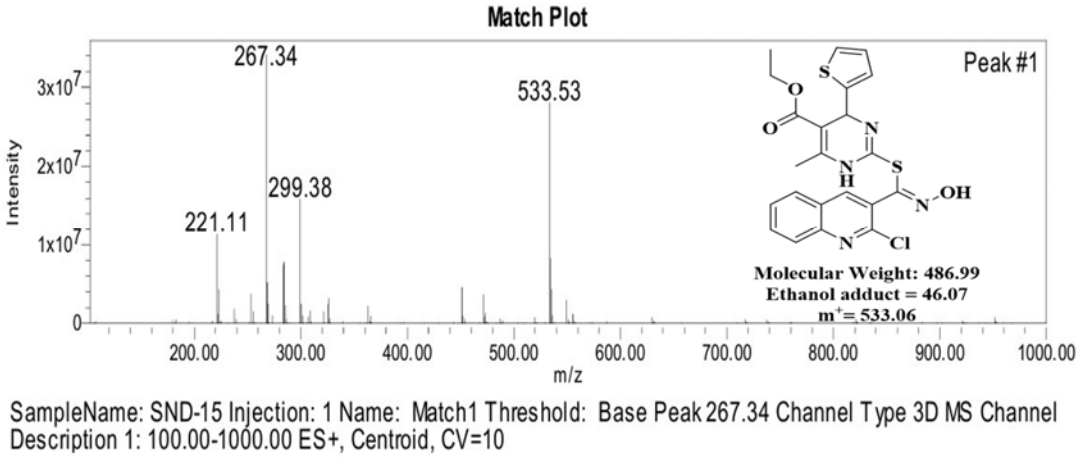

Figure 9: Mass spectrum of compound **6c**

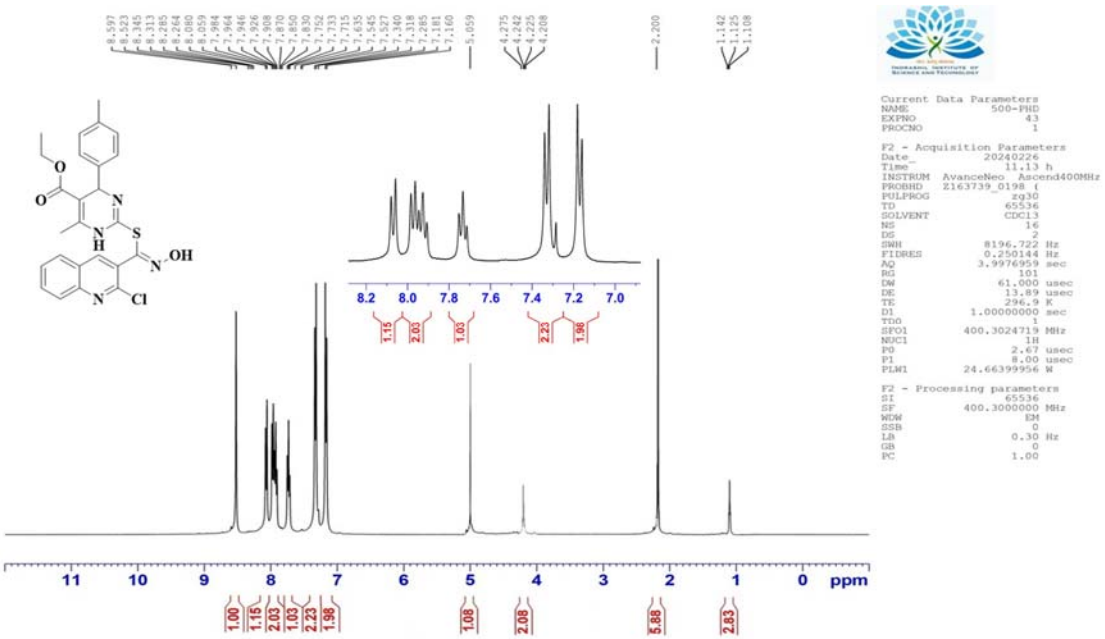

Figure 10: ^{1}H NMR of compound **6d**

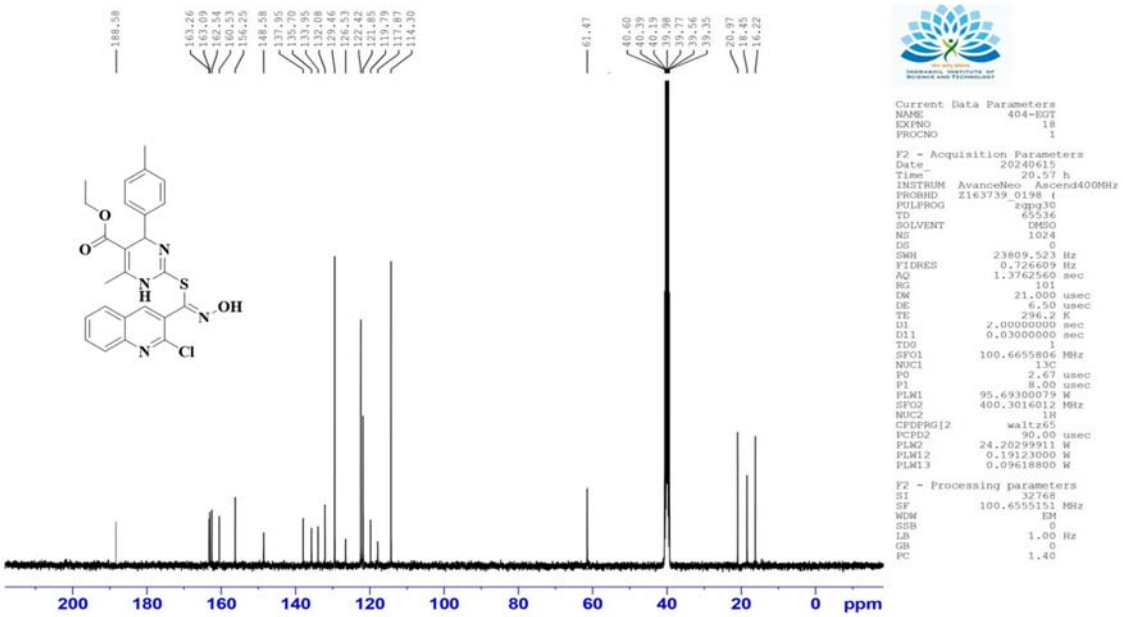

Figure 11: ^{13}C NMR of compound **6d**

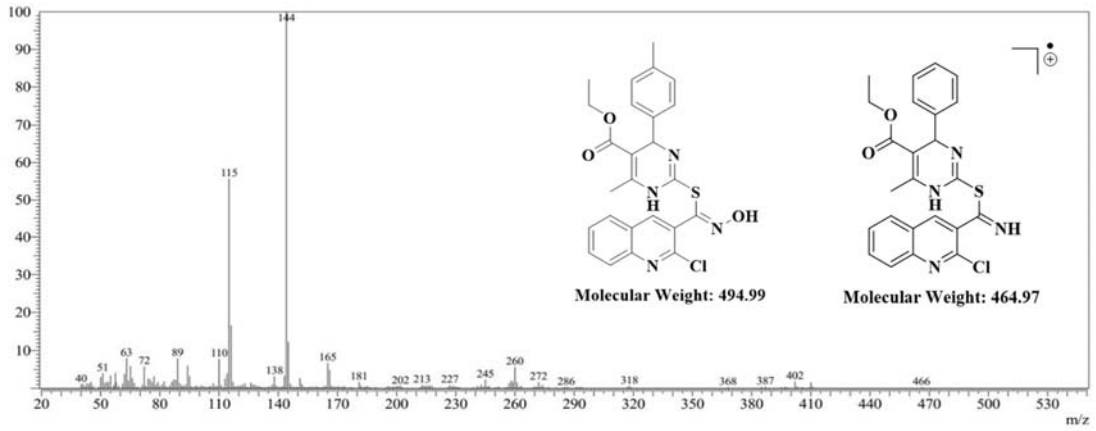

Figure 12: Mass spectrum of compound **6d**

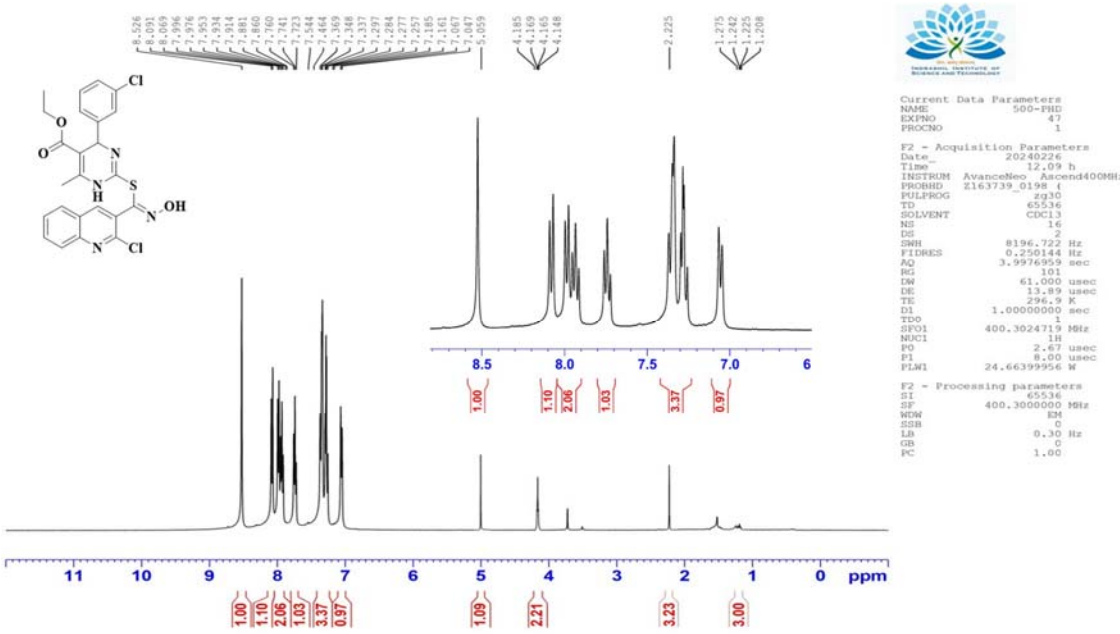

Figure 13: ^{1}H NMR of compound **6e**

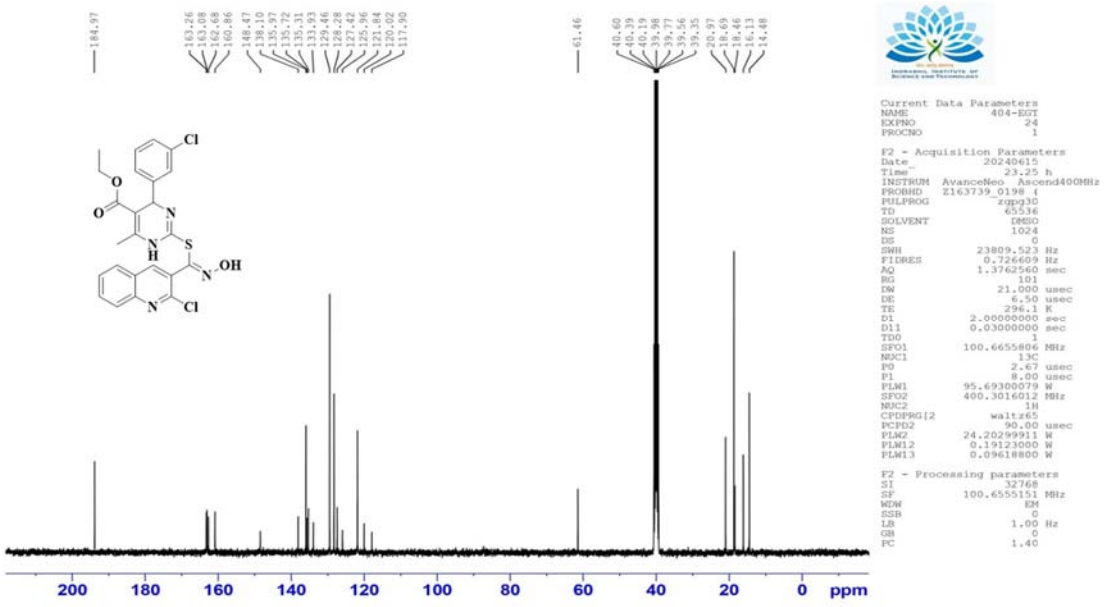

Figure 14: ^{13}C NMR of compound **6e**

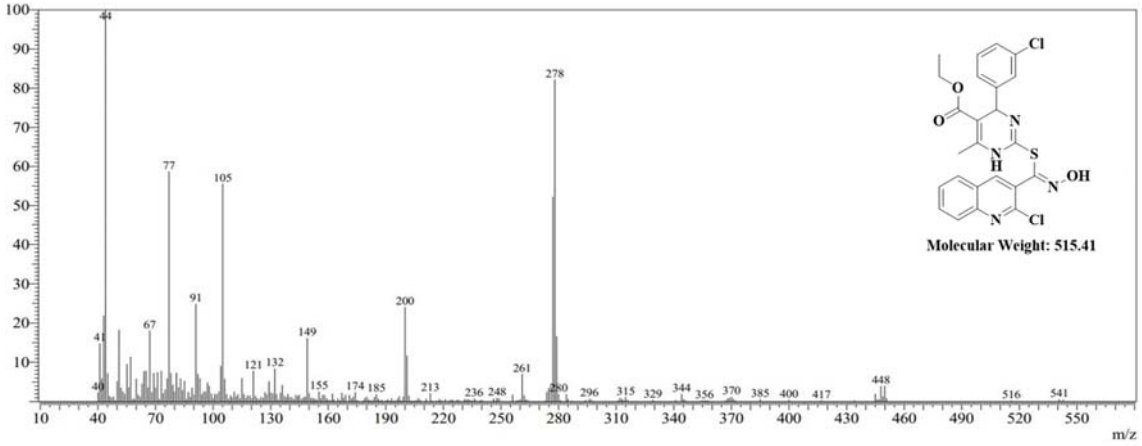

Figure 15: Mass spectrum of compound **6e**

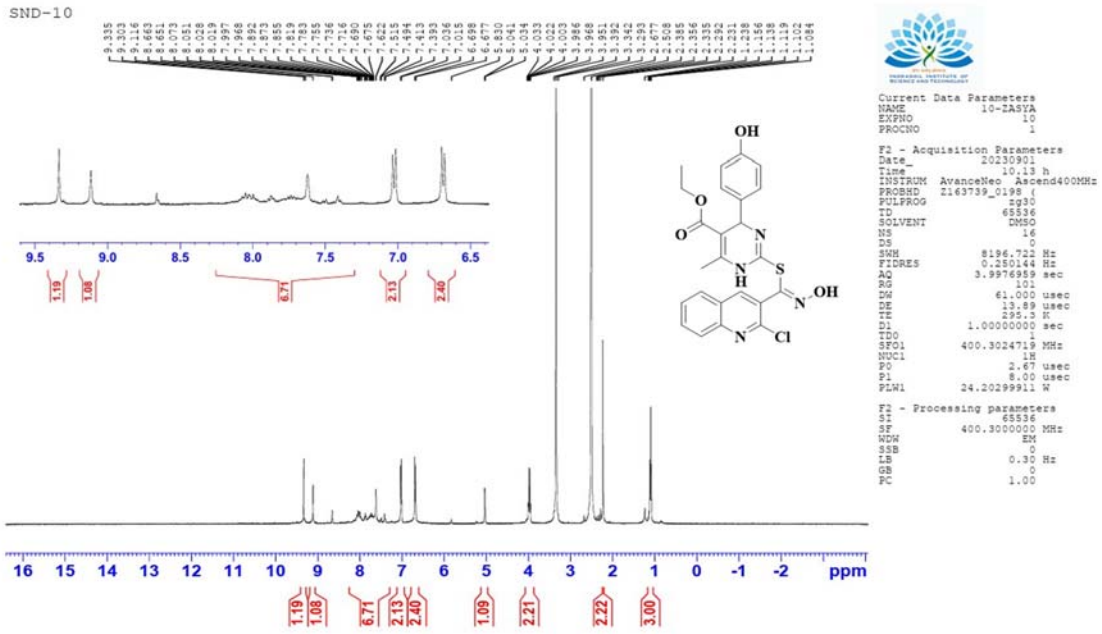

Figure 16: ^{1}H NMR of compound **6f**

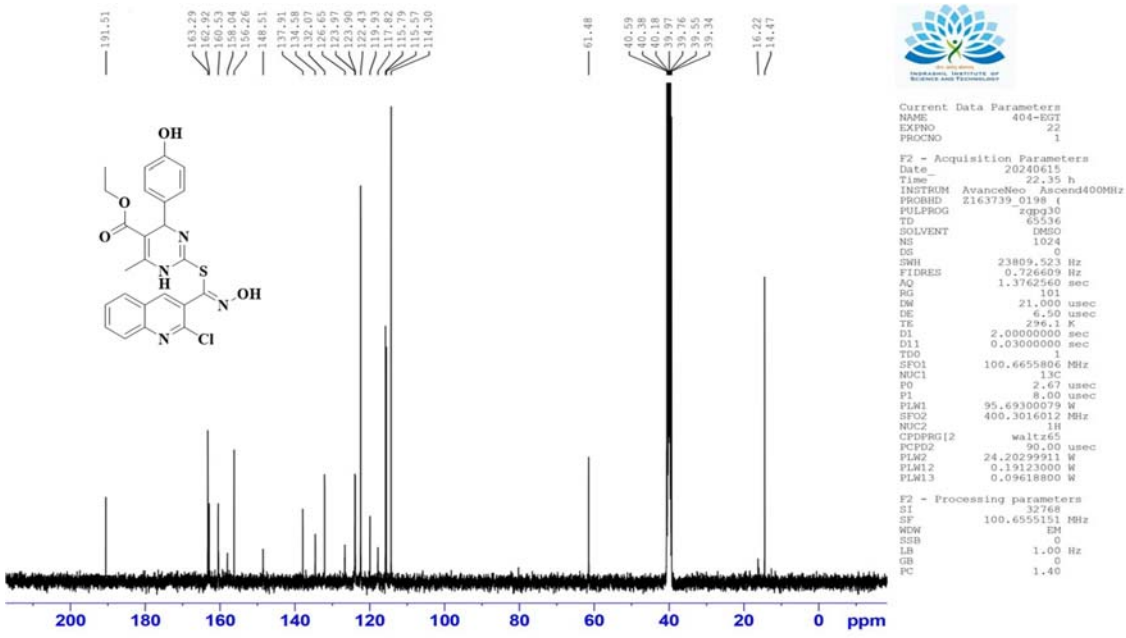

Figure 17: ^{13}C NMR of compound **6f**

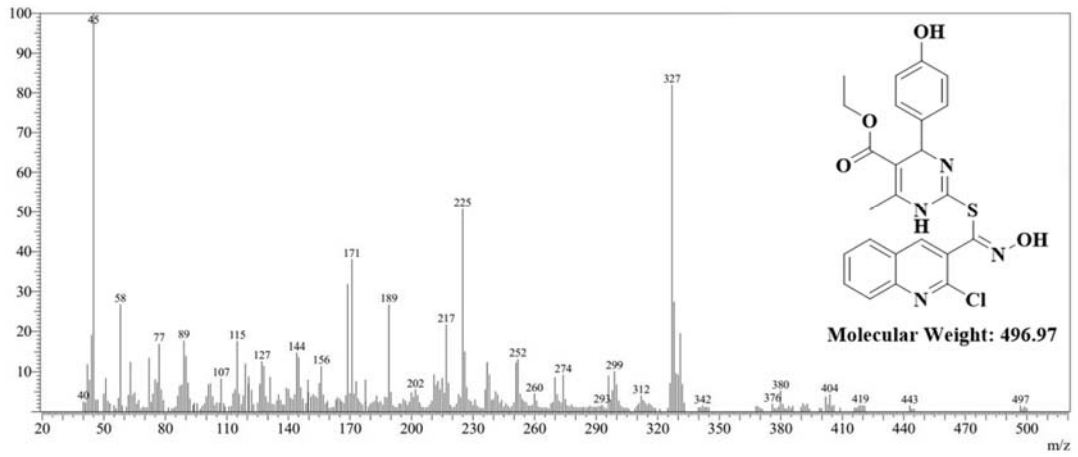

Figure 18: Mass spectrum of compound **6f**

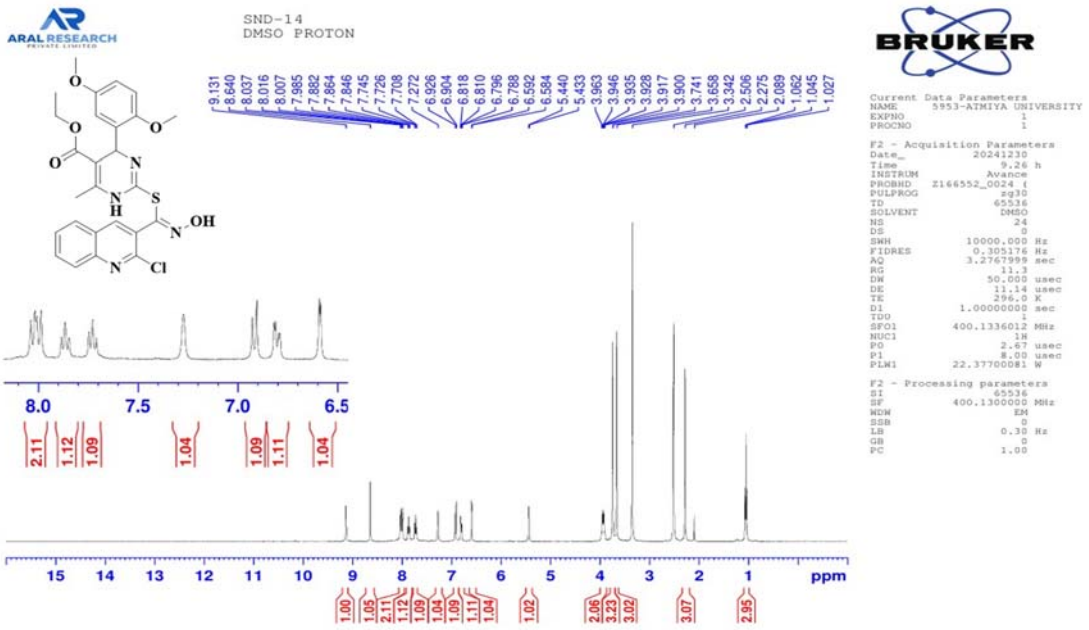

Figure 19: ^{1}H NMR of compound **6g**

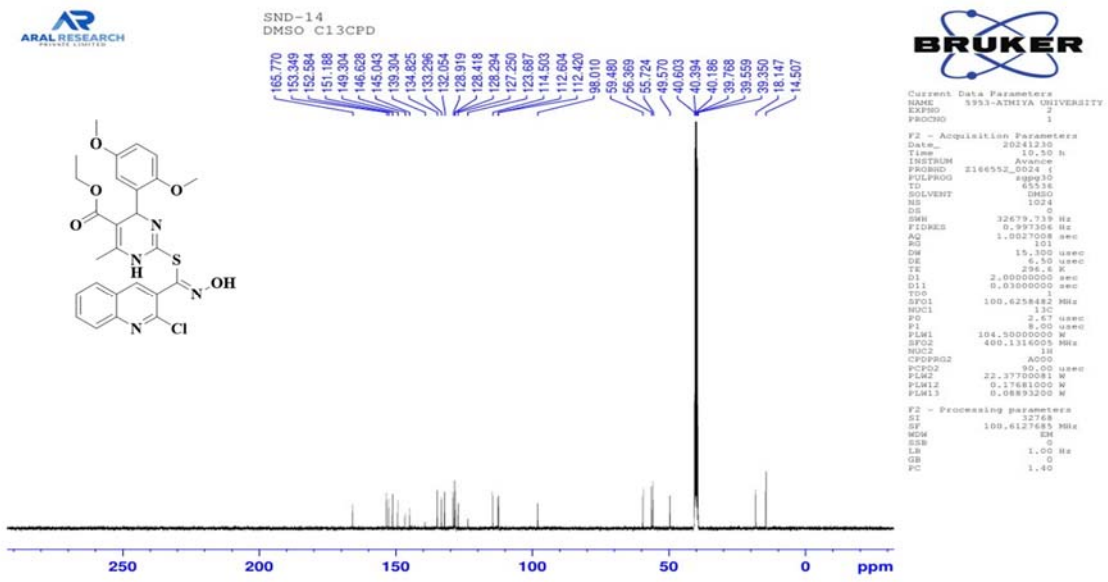

Figure 20: ^{13}C NMR of compound **6g**

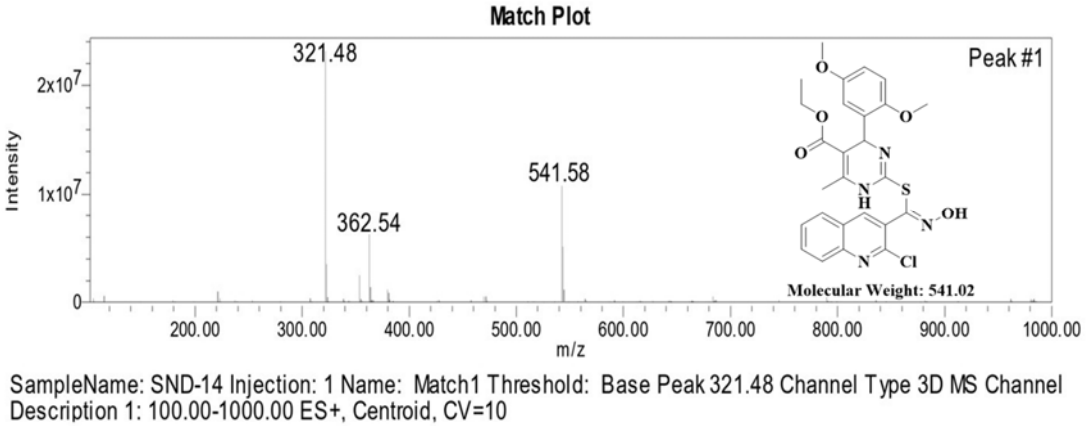

Figure 21: Mass spectrum of compound **6g**

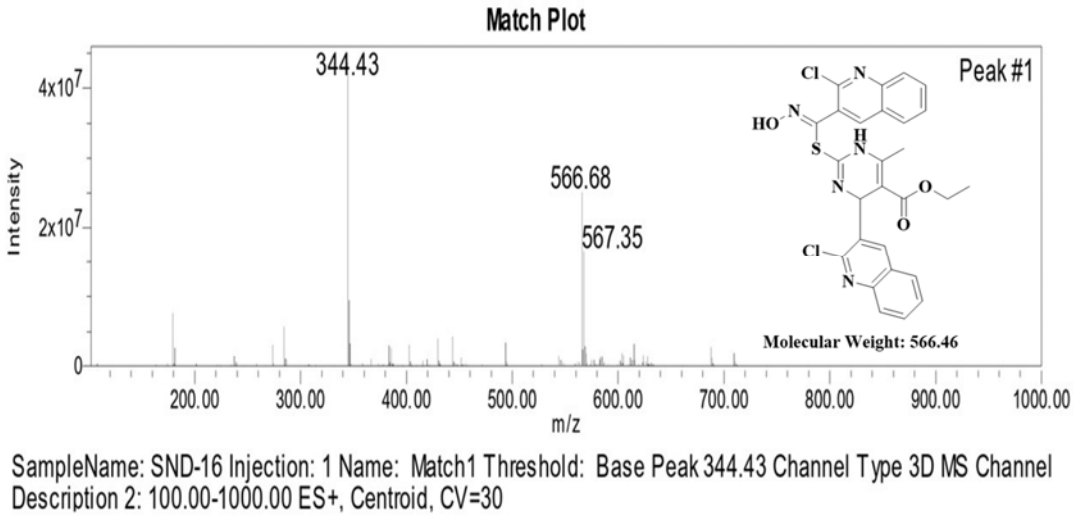

Figure 22: Mass spectrum of compound **6h**

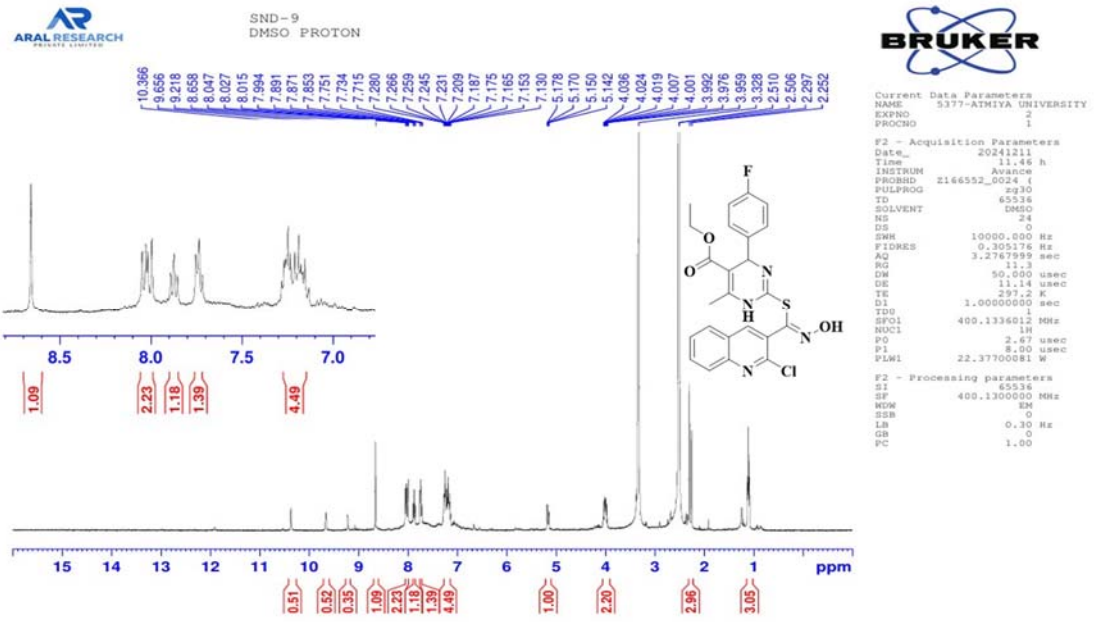

Figure 23: ^{1}H NMR of compound **6i**

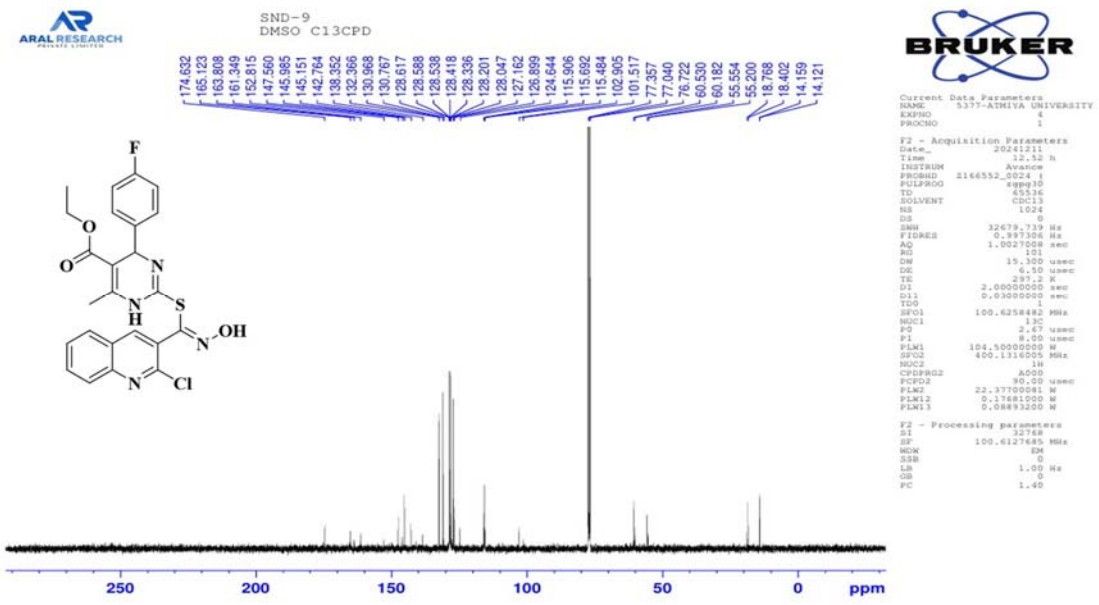

Figure 24: ^{13}C NMR of compound **6i**

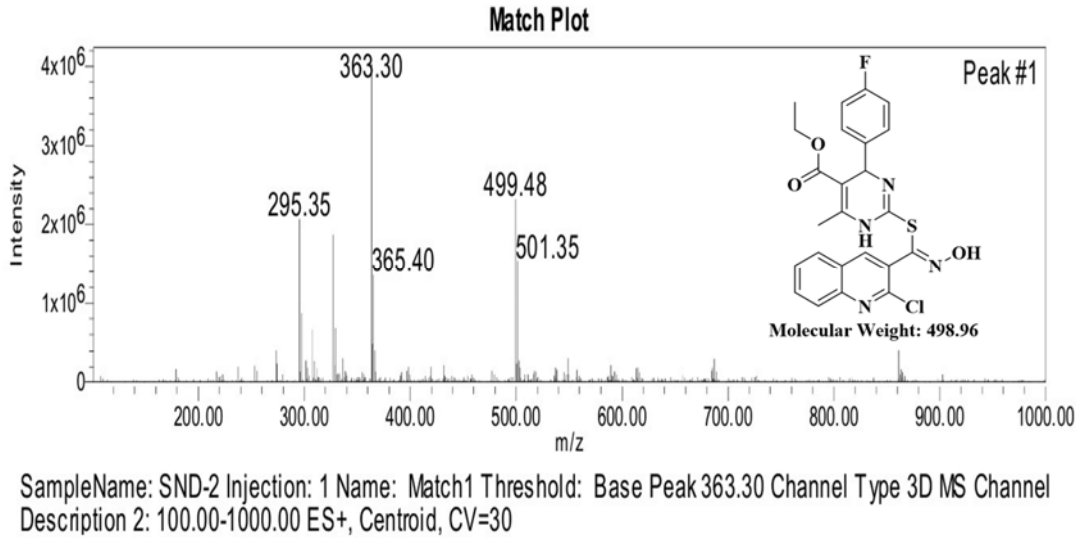

Figure 25: Mass spectrum of compound **6i**

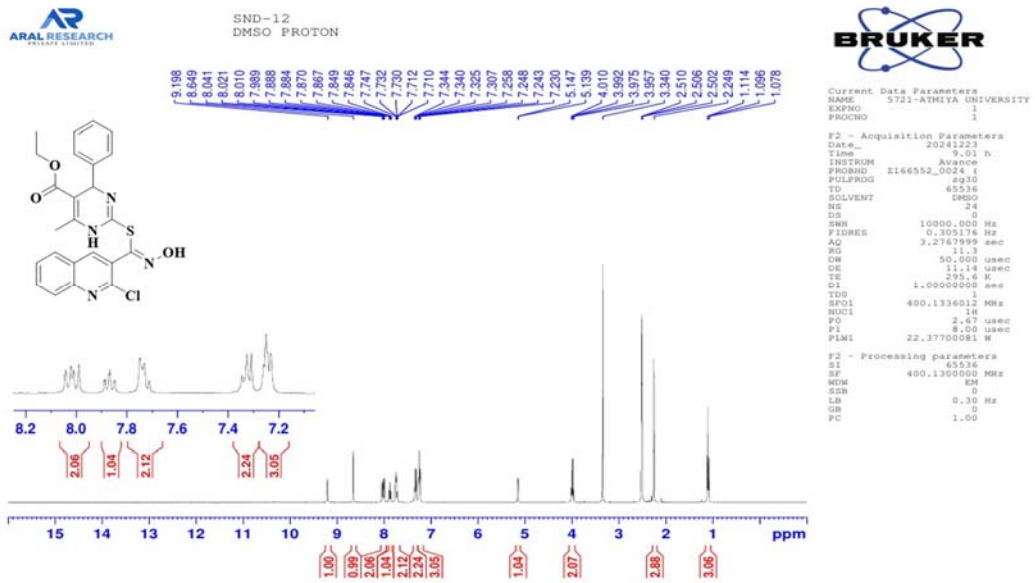

Figure 26: ^{1}H NMR of compound **6j**

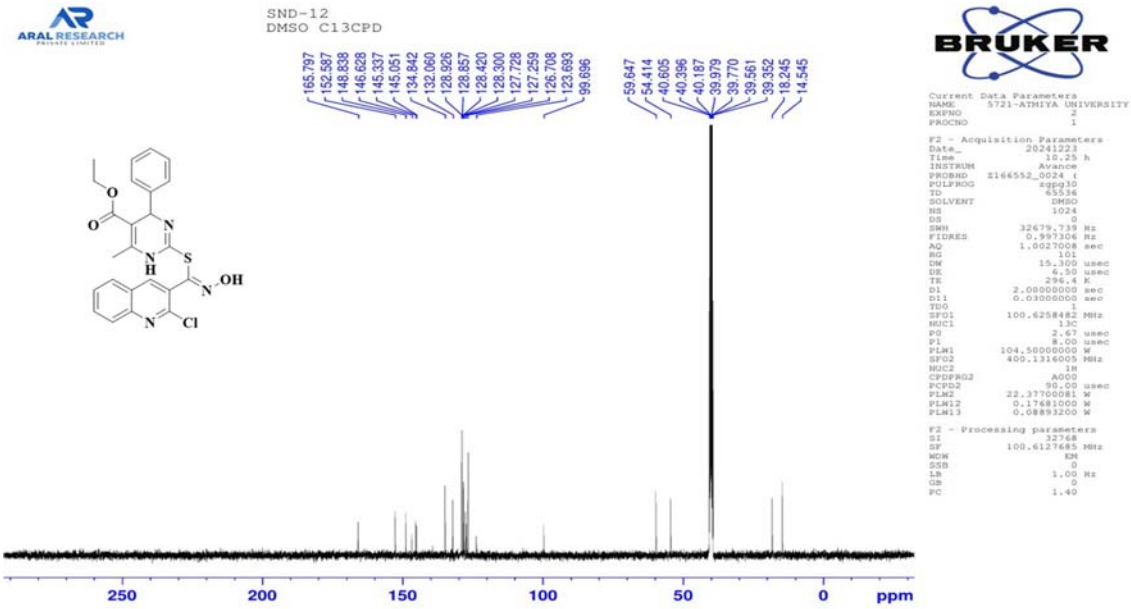

Figure 27: ^{13}C NMR of compound **6j**